University of Fort Hare
Together in Excellence

MONITORING THE IMPACT OF DEFORESTATION ON AN AQUATIC ECOSYSTEM USING REMOTE SENSING: A CASE STUDY OF THE MNGAZANA MANGROVE FOREST IN THE EASTERN CAPE PROVINCE

BY
Madasa Akhona
(**201406466**)

Submitted in fulfilment of the requirements for the degree of
MSc in Applied RS & GIS
Faculty of Science and Agriculture
University of Fort Hare

DECEMBER 2020

SUPERVISED BY
Mr P. C. Sibandze

DECLARATION

By submitting this dissertation, I declare that the entirety of the work contained herein is my own original work that I have not previously, in its entirety or part. submitted for obtaining any qualification.

Signature: 

Date: 09 March 2021

ABSTRACT

Coastal mangrove vegetation at Mngazana continues to be threatened and reduced periodically due to unmonitored harvesting. Covering an area of 148ha, the Mngazana mangrove forest remains unreserved, thus, research on the Mngazana mangroves is essential in order to monitor their state and sustainable management. Since in-situ monitoring of mangrove areas is both challenging and time-consuming, remote sensing technologies have been used to monitor these ecosystems. This study was carried out to monitor the impact of deforestation using ASTER satellite images over ten years: from 2008 - 2018. Validation was carried out by comparing classification results with the ground-referenced data, which yielded satisfactory agreement, with an overall accuracy of 94.64% and Kappa coefficient of 0.93 for 2008; and in 2009, the overall accuracy was 88.62% and a Kappa coefficient of 0.85. While the overall accuracy of 95.08% and a Kappa coefficient of 0.92 for 2016 and 2018 were observed, the overall accuracy of 93.58% and a Kappa coefficient of 0.91 was yielded. NDVI and SAVI indices were used as monitoring indicators. The results obtained in the study indicated that the canopy density of the mangrove forest remained unchanged in the years under investigation. However, insignificant changes in canopy density were identified between 2009 and 2016.

KEYWORDS

Mangroves, ASTER, Normalized Difference Vegetation Index (NDVI), Soil Adjusted Vegetation Index (SAVI), Remote Sensing, Vegetation Indices, Mngazana

ACKNOWLEDGEMENTS

I would like to thank uMfihlakalo, Umvel'iQangi, uQamata and my Ancestors oNxasana oSikhonza, for giving me the strength and patience every day and constantly reminding me that giving up is not an option.

A special thanks go to my supervisor Mr Phila Sibandze for all the support, input and pushing me to do well in my studies. Thank you for not giving up on me.
The financial support I got from SAIAB and CSIR made this possible. I am very grateful.

My family has been my pillar of strength throughout this journey, the words of encouragement you always give me led to this, and I am forever grateful for the support and love and having faith in me. Thank you, Mom, Yaya, Ta Si, Madcat, Riri, Samie, Elona, Mangara, Soso and Toto.

My colleagues and friends were my backbone on this journey, from field data collection to sleeping at the lab to cross-night. Guys I appreciate you; Oscar, Mihle, Nasie, Pam, Phila, Siyavuya, Omega, Rochen, Zama, Madoda, Fulu, Dr Isreal, Somthi, Kwata, Martins, Godfrey, Qelisile, Bornwell, Vuyo, Mnce, Bruce, Unathi, Nonkula, Sidondi, Mzondi, Mgidlana, Pangumso, Odwa, Dida, Admire and my late friend Yonela Boli.

To Dr Olusola Ololade, thank you, my Mentor, for constantly pushing me, for still making me believe in myself. I have gained much confidence under your mentorship, thank you for everything, this would not have been possible without your hand.

Lastly, I want to thank my church for the prayers and words of wisdom. When I was down, you lifted my spirit, and you reminded me of the powers I have. Thank you for the strength neNtsebenzo Zulu.

CONTENTS

TABLES

FIGURES

ACRONYMS AND ABBREVIATIONS

ASTER	Advanced Spaceborne Thermal Emission and Reflection Radiometer
LAI	Leaf Area Index
MLC	Maximum Likelihood Classification
NDVI	Normalized Difference Vegetation Index
NIR	Near-Infrared
SAVI	Soil Adjusted Vegetation Index
VNIR	Visible Near Infrared

1. CHAPTER 1

1.1. INTRODUCTION

Mangroves are considered one of many tropical, sub-tropic and temperate regions that play a significant role in occupying a variety of settings inclusive of estuarine environments, inlets, and islands (Alongi, 2008). In contrast, Duke and Larkum (2019) defined mangroves as a diverse group of predominantly tropical trees and shrubs that grow in half of the intertidal zones of coastal areas worldwide. Mangroves serve an essential role within the ecosystems at which they exist; they stabilize the coastline by rapid colonization of substrates, thereby trapping subsequent sediments with their roots, which in turn leads to mud and or sand formation in areas, which makes further colonization to take place.

According to Quoc Vo et al. (2015), mangrove forests can dominate estuaries' intertidal zones together with shorelines along many of the world's tropical and subtropical coastlines. They are also dependant on the shorelines, which are sheltered by coral reef structures, which protect the sediment-sensitive corals against materials received which are not wanted to be flushed downstream from the surrounding land catchment. (Pastor-Guzman et al., 2018) illustrated that mangroves are ecosystems that are taxonomically diverse in the assemblage of tree species which have common morphological, biochemical, physiological and reproductive adaptions that allow them to colonize and develop in environments of high saline hypoxia.

Within an estuary environment, mangrove forests are distributed in inter-tidal regions between the sea and the land, and, they grow in tropical and subtropical latitudes, which is the region between the 30°N and 30°S latitudes. Their distribution is limited by significant ocean currents and isotherms of seawater in winter having 20°C temperatures, and, their distribution is from the mean sea level to the higher spring tide (Giri et al., 2011; Alongi, 2009).

There are nine orders, twenty families, twenty-seven general families and seventy species of mangroves. They grow in harsh environments comprised of high tides, muddy anaerobic soils, and an element between terrestrial and marine ecosystems.

Mangroves are crucial because they serve as the most productive carbon marine ecosystem by contributing to carbon found in the coastal ocean, although they constitute a small percentage of the land cover compared to the global coverage (Alongi et al., 2012; Lavieren et al., 2012.) The global scope of mangrove forests mapped from tropical and sub-tropical regions is estimated to be about 150 000$km^{2.}$. This is 1% less than all the tropical forests globally, which is also less than 0.4% of the total global forests.

In South Africa, mangrove forests are mostly distributed in estuaries from Kosi Bay in KwaZulu Natal (KZN) to Nahoon estuary, located in the Eastern Cape. (Rajkaran, 2011), (Figure 1.) The Mngazana estuary is an essential source of mangrove litter and particulate organic carbon for the marine environment adjacent to it, which is suitable for sustaining the nearshore's food webs (Rajkaran & Adams 2007). Mangroves offer many functions to both marine and land animals. Fishes, prawns, shrimps, crabs, oysters, mussels and cockles use mangroves as nurseries and breeding grounds.

The local population use mangrove forests as their source of firewood, building material for recreational activities such as boating, canoeing, fishing and collecting molluscs (Ghosh et al., 2016), whilst, birds use these tree’s canopy for roosting; shellfish use the roots to attach themselves; fish use mangroves as a breeding ground and bats and honeybees use them as their source of nectar (Lavieren et al., 2012). They are ecological and economically viable offering goods and services; such as coastal protection to communities, food security and they are rich in biodiversity.

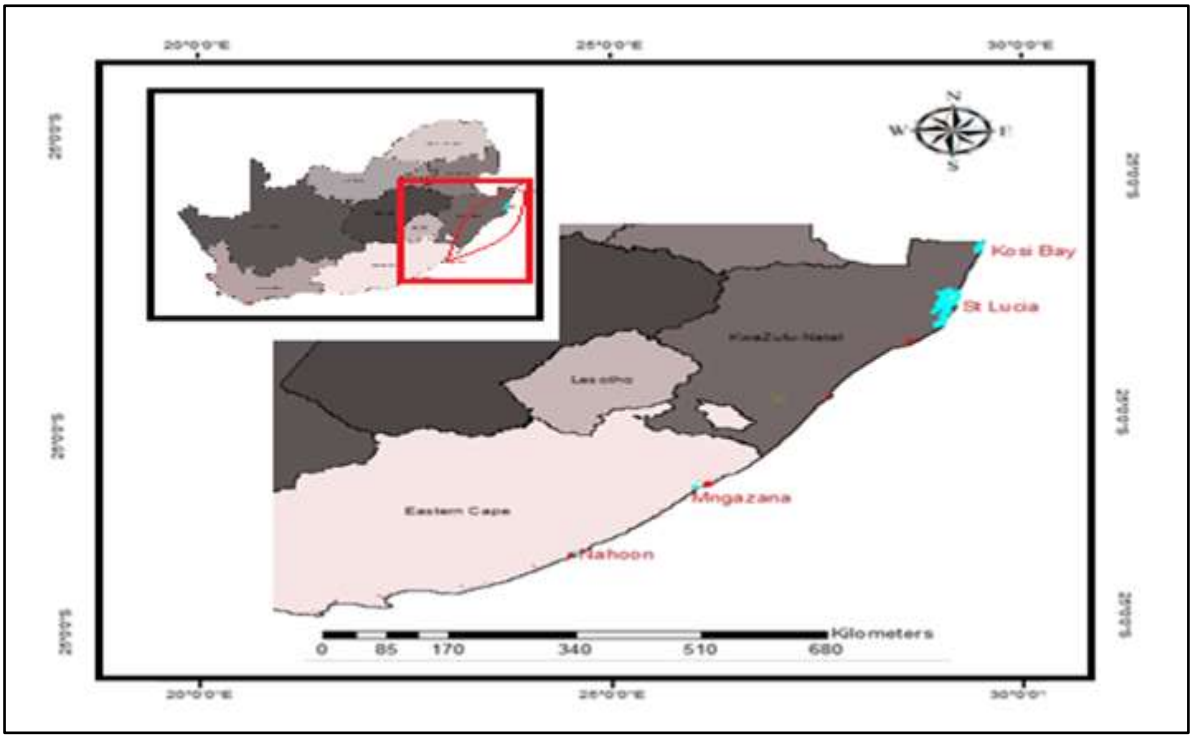

Figure 1: Distribution of mangroves along the East Coast of South Africa, from Kosi Bay to Nahoon Including the Study Area, Mngazana Estuary

Since mangrove forests are a highly effective world's carbon storage and sink; along with their living biomass, the mangrove soils are carbon-rich because mangroves sequestrate carbon for a thousand timescales. Lavieren et al. (2012) found that mangroves are ecosystems that shape, build and maintain the legacy of their surrounding's physical environment. When observing mangroves, the most striking feature is that they grow in harsh environments characterized by extreme saline conditions and flooding on the one side and aridity with lowland vegetation on the other side (Lavieren et al., 2012).

Sediments where mangroves are comprised of soft waterlogged and unstable physical factors such as chemical composition, salinity, soil acidity, substratum and climatic conditions, shape their development, growth, and productivity. Deforestation, especially in the tropics and subtropical areas, is the second largest recorded source of Carbon Dioxide (CO_2) following fossil fuels and contributing to about 12-20% of the total deforestation (Hutchison et al., 2014).

Demand for mangrove forest resources has led to a decrease in mangrove species over the past century. Aquaculture, agriculture and urbanization are the main factors contributing to the deforestation of mangroves. Recent estimations of mangrove deforestation, according to Lagomasino et al., (2019) indicate that they range between 0.16% to 0.39% per year at regional and global scales. In

this regard, mangroves are highly threatened species; about a third of the world's mangroves have declined over the past five decades, the rates estimated for annual deforestation were at 0.7% from 2000-2005; higher than or similar to those tropical forests which are three times higher than the mean rates for forest loss globally (Alongi, 2002).

Despite the declining rates combined with high carbon values, mangroves may contribute 10% of the total carbon emission from deforestation (Donato et al., 2011). Loss of mangroves is continuing in most areas; and, regardless of their declining rate, mangroves are still endangered at about 3 to 5 times as faster as overall global forest losses. Some countries have lost more than 40% of their mangrove area over a 25-year period, and only degraded areas have remained (Lavieren et al., 2012). If this trend continues, mangrove forests will have an ecological and socio-economic impact, especially in communities dependent on mangrove for resources such as food, fuel or coastal protection.

Research has indicated that the global population of mangroves is declining over the years, yet they play a vital role in both the marine environment and the local communities in which they exist. It is therefore essential to monitor mangrove forest spatial distribution and dynamics over time. However, researching in line with mapping and monitoring mangrove forests can be challenging when collecting field data. It is not easy to determine the distribution of mangroves, however abundant they are in the field, due to their inaccessibility within their communities; therefore, Remote Sensing is the technology that provides the means to address this challenge as it allows for methods proven efficient for mapping and monitoring mangrove forest (Zhang et al., 2017).

Remote Sensing is a technology based on satellites used to gain knowledge of an object's features or properties without making physical contact with those features or items of interest. Such technology is not limited to mapping vegetation covering large areas because it can also focus on areas underwater, thereby mapping aquatic vegetation, which is the decisive indicator of marine and freshwater ecosystems (Blanco, 2013).

Nevertheless, remote sensing does have limitations, especially when used for aquatic mapping of vegetation, unlike detecting terrestrial vegetation. These limitations are due to dominant water reflectance and differentiation of

submerged species (Blanco, 2013). On the other hand, Jung et al., (2012) argues that cases associated with aquatic remote sensing result in a situation where the total signal received by the Satellite Sensor is dominated by radiance contributed by atmospheric scattering and only about 8% to 10%.

1.2. PROBLEM STATEMENT

In South Africa, threats to mangroves involve wood harvesting, altered water flow patterns coupled with salinity changes, and conditions associated with prolonged closed-mouth and subsequent modifications to the intertidal habitat (Rajkaran, 2011). At Mngazana estuary, wood harvesting is the main reason the mangrove density is on the decline. Rajkaran and Adams., (2007) estimated that wood harvesting is happening at a rate of 1 ha per year and if this trend continues with no regrowth, after 118 years, there will be no mangrove forest in Mangazana. Hoppe-Speer et al., (2015) argued that the Mngazana mangrove forest is decreasing over the years. Observation indicated that the forest was 150 ha in 1982, 145 ha in 1999 and 118 ha in 2012. Therefore, this suggests a 27 ha or a 19% decrease in Mngazana forest in three decades.

This research study will therefore assess the spatial and temporal changes at the Mngazana mangrove forest using remote sensing techniques by using vegetation indices as indicators. These indices will be calculated and studied to provide a long-term account of the change dynamics driving the spatial decline observed in the forest over the years. As a result, the investigation will focus on ten years, from 2008 to 2018.

1.3. HYPOTHESIS

Mngazana mangrove forest has been declining over the past four decades and the rate of change has been accelerating exponentially due to anthropogenic activities.

1.4. OBJECTIVES

1. Identification of mangroves from surrounding landcover at Mngazana mangrove forest using ASTER data.
2. Mapping and monitoring the rate of change at the Mngazana mangrove forest from 2008 to 2018.

3. To investigate whether deforestation has taken place at Mngazana mangrove forest using NDVI, LAI & SAVI.

1.5. STUDY AREA

This study was conducted at Mngazana, a permanently open estuary situated in the Eastern Cape Province, 18kms south of Port St Johns; surrounded by three communities: Cwebeni, Thekweni, and Mquleni (Figure 2). The Mngazana area has a warm subtropical climate characterized by air masses usually unstable, and these are the main reason for the rainfall all year out. Annual rainfall averages range from 75-150 cm, while thunderstorms during summer and precipitation caused by frontal rain are expected. In summer, mean monthly temperatures range around 27°C, and during winter, they range around 5°-12°C; this is a small daily range of temperatures (Peter sen et al., 2010). The Mngazana area receives an average of 1200 mm of rain per year, and about 70% of the rainfall occurs in summer (Traynor, C H, and R, 2008).

The minimum and maximum air temperatures range from 16–20°C and 23–26°C per annum respectively, whereas wind velocities were notably uniform over fifty-four years ranging between 4 and 5m s–1 (Rajkaran. & Adams., 2007). The Mngazana mangroves are the third-largest in the country, and are found within the Mngazana estuary. It covers 118ha, which is 67% of the Mngazana plant community (Colloty 2000). There are three mangrove species found within the estuary: Avicennia Marina (Forssk. Vierh.), Bruguiera Gymnorrhiza (L.) Lam and Rhizophora Mucronata Lam (Rajkaran. & Adams., 2007). The estuary is estimated to be 5.3km in length, situated at the Mngazana river's mouth, which stretches for 150km within a catchment area of 275km2 (Branch & Grindley, 1979). In the middle reaches of the estuary (1 085m from the mouth) and the lower reaches (300m from the mouth), there are two creeks fringed by large populations of mangroves (Branch & Grindley, 1979).

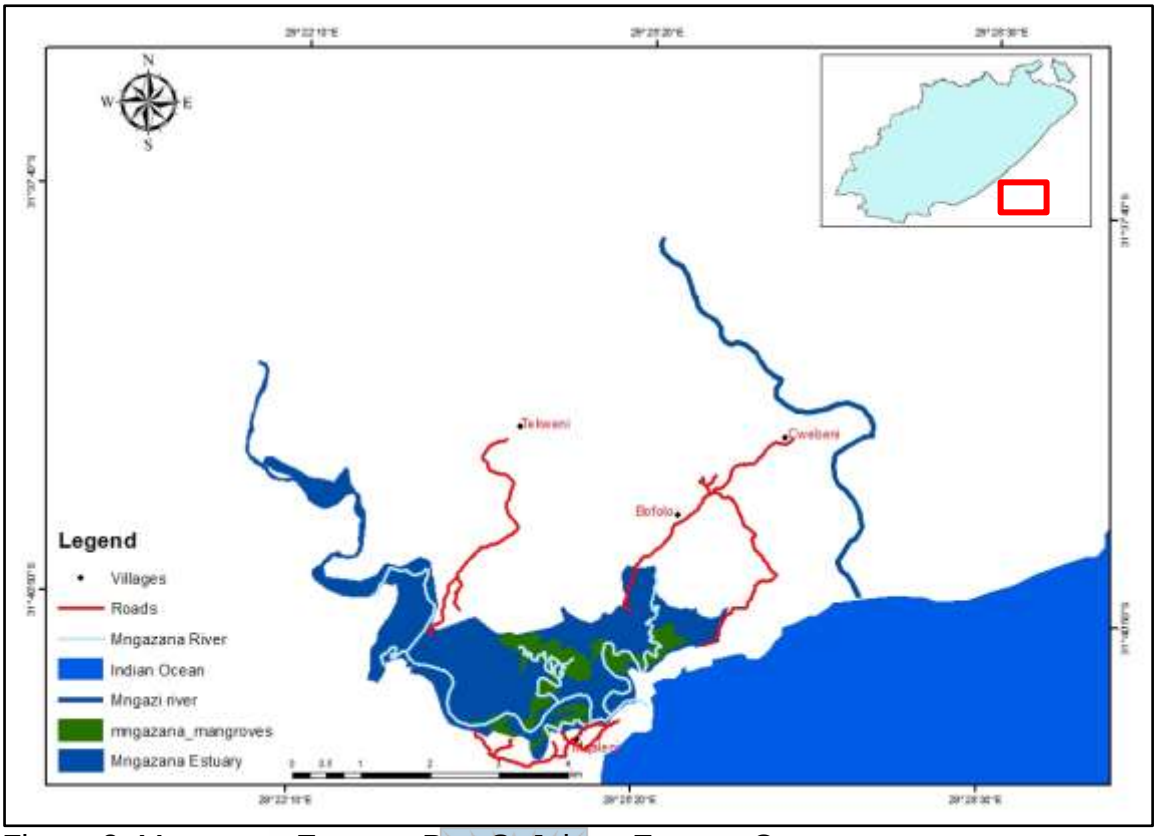

Figure 2: Mngazana Estuary, Port St Johns, Eastern Cape.

1.6. RESEARCH QUESTION

Can remote sensing using ASTER satellite imagery be capable of mapping and monitoring the deforestation occurring at Mngazana mangrove forest?

2. CHAPTER 2: LITERATURE REVIEW

2.1. INTRODUCTION TO REMOTE SENSING OF MANGROVES

Remote Sensing has been used to map and monitor the earth's surface because of its capability to map areas that are not physically accessible. Scholars and researchers alike have used such capabilities in different disciplines such as environmental studies, hydrological mapping, mineral exploration; and cause marine studies, including mangrove mapping and monitoring. The use of remote sensing technology in mangrove mapping started as far back as the 1980s where Terchunian et al., (1986) was conducted a study to create historical maps of the mangrove's ecosystem in Ecuador. Though the technology was relatively basic at the time, the outcomes of the study indicated that Landsat, airborne MSS, radar and aerial photographs, managed to map the mangroves.

As the number of earth observation satellites increased in space, this subsequently provided a wide range of data available to researchers to develop and investigate a range of techniques in studying mangroves. In 1992 (Gang & Agatsiva, 1992) conducted a study in Mida Creeks, Kenya, using SPOT multispectral satellite imagery to map the mangroves covering an area of 890 ha, which was 15.9% of that forest, while Pasqualini et al., (1999) used SPOT-XS data, to map the alterations of aquaculture farming in mangroves in the coastal marsh of Mahajamba (North-Western Madagascar). In 1997 Venkataratnam et al., (1997) used Landsat to map mangroves in the coastal areas of Andhra Pradesh, India, while L. Wang et al., (2004) used a combination of IKONOS 1m panchromatic and 4m multispectral images to map mangroves in a study located at Punta Galeta on the Caribbean coast of Panama. Therefore, the aforementioned is evidence that scholars realized the importance of using remote sensing techniques in studying mangroves hence different sensors and algorithms have been used to map and monitor mangroves in other parts of the world. Furthermore, this also proved the potential and importance of utilizing satellite-based information mangroves studies.

Further, remote sensing has also been used in canopy distribution, biomass, extent and classification. A few studies have used remote sensing to map and monitor mangrove forests using different remote sensing data types. Some studies have used hyperspectral and optical data with medium to high spatial resolution for mapping mangroves (Green et al., 1998; Held et al., 2003; Le Wang et al., 2004; Neukermans et al., 2003), while other studies have demonstrated the potential of mangrove mapping using radar data (Kuenzer et al., 2011; Lucas et al., 2007). SAR data has also shown successes in mapping mangroves (Fatoyinbo & Simard, 2013; Held et al., 2003; Lucas et al., 2009; Mougin et al., 1999; Proisy et al., 2000; Proisy et al., 2002; Simard et al., 2006). Shuttle Radar Topographic Mission (SRTM) has proved to be capable of estimating canopy height and mangroves' biomass (Fatoyinbo et al., 2008; Fatoyinbo & Simard, 2013; Simard et al., 2006; Simard et al., 2008). Some studies have applied a hybrid approach by combining SAR and optical remote sensing data for mangrove mapping with promising results (Aschbacher et al., 1995; Held et al., 2003).

2.2. SPATIAL DISTRIBUTION OF MANGROVES IN SOUTH AFRICA

Mangroves are an intertidal zone of woody plants located in the world's tropical and subtropical regions. They are by far the most productive forest ecosystem, having a marine and being terrestrial unique in the world. In South Africa (SA), mangroves' spatial distribution is limited to the protection of estuaries having low energy from those that are high in energy in the coastline and where embayment has diluted freshwater from the rivers (Rajkaran & Adams., 2007). The total coverage of mangroves in South Africa was estimated to be about 1 631 ha, with less than 1% covering the total land area and the most minor and rare forest type in the country (Rajkaran et al., 2010). Mangroves are limited to the country's East Coast between the Great Kei River and Kosi Bay in the North Coast Figure 3.

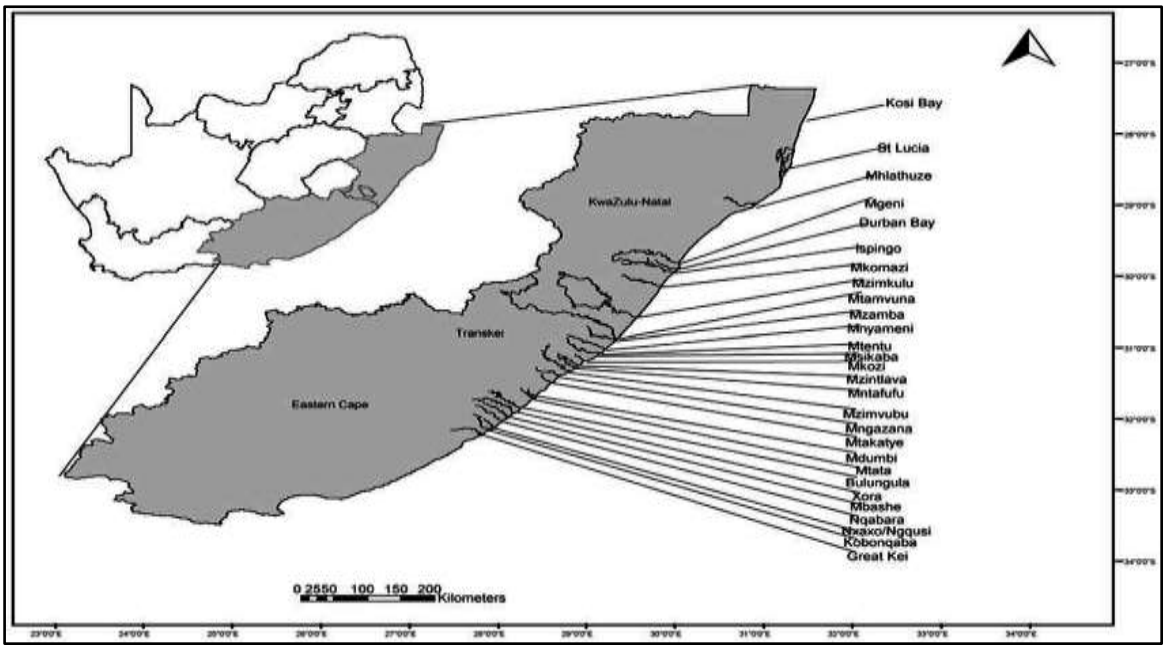

Figure 3: Mangrove distribution along the East Coast (Adam et al. 2003)

Mangroves in South Africa stretch from Kosi Bay's forest in KwaZulu-Natal to Nahoon Estuary in the Eastern Cape, as indicated in Figure 3 above. These mangroves vary in sizes; the largest is Mhlathuze with 652.1 ha, followed by St Lucia with 571.0 ha and the third-largest being Mngazana mangroves forest with 150 ha (Rajkaran & Adams, 2012). According to Traynor et al., (2008), the Wild Coast in the Eastern Cape is covered by dynamic mangroves, and it has been reported that the loss of mangroves in that area was about 6.5% over a seventeen-year period. Rajkaran et al. (2004) highlighted that only six types of mangroves species were found in the country, with Lumnitzera Racemosa Willd, Ceriops Tagal Perr, C.B. Robinson and Xylocarpus Granatum Koen found only in Kosi Bay, the southern distribution limit of tropical species.

Avicennia Marina (Forsk. Vierh.) and Bruguiera Gymnorrhiza (L.) Lam is commonly found in most South African estuaries where there is a presence of mangroves, while Rhizophora Mucronata occasionally occurs from Kosi to the Bulungula River in the Eastern Cape. The Rhizophora Mucronata species are found in ten of the thirty-seven mangrove estuaries along the eastern coastline, of which four of those places are in the Eastern Cape (Yang et al., 2018).

South Africa consists of 0.05% of Africa's total mangrove coverage area, an almost insignificant amount, however this particular type of forest in South Africa contributes to the country's rich biodiversity (Rajkaran & Adams, 2010). The extent of mangroves on the eastern coastline decreases from the northern parts to the south; hence northern estuaries have the largest estuaries compared to mangroves based in the south, with the Mhlathuze estuary having 80% coverage of the total mangrove area (Rajkaran et al., 2004).

From the above discussions, the spatial distribution of mangroves in South Africa evidently leans towards the country's eastern area. One has to ask a question, "What are the driving factors that contribute to such an occurrence? Why are there no mangroves on the West Coast"? Could it be climatic conditions between these two areas of the country, as it is well known and document that the east enjoys a tropical climate while the west is characterized by a Mediterranean kind of climate (Naidoo, 2016)? Further studies have to be conducted to understand such a phenomenon fully.

2.3. SOCIO-ECONOMIC IMPORTANCE OF MANGROVES ECOSYSTEM

Mangroves contribute both socially and economically to livelihoods in the communities in which they are found. They provide them with building material for dwellings, building kraals, as well as fuel. Although most mangrove species are under the threat of extinction due to being over logged and deforestation, there is still a need to protect this essential marine and bio-sensitive ecosystem. Mangroves play a critical role in stabilizing near-shore sediments that help prevent coastal erosion, and they also act as nurseries for numerous marine species such as shrimp and fish in their early life stages (IUCN 2017). On the other hand, mangroves also have a social benefit as well; they provide the communities with wood as a building material, which is also resistant to insects and decay.

Many coastal indigenous communities rely on this wood for construction material, fuel and use the mangrove trees for medicinal purposes. Recently, the forests have also been harvested commercially for pulp, wood chips, and charcoal production to build houses and firewood (Duke 2019). Since mangroves are a habitat to many fish species that use them as breeding grounds and nurseries for many fish species, it is easier for coastal communities to go fishing and provide themselves with food. Legal (commercial) fishing contributes to the economy, unlike illegal (subsistence) fishing, where people do not have permits for fishing. In addition, about 75% of commercially caught fish may inhabit mangroves at some point in their life (Bangman, 2007).

The role of mangroves in many communities is filtering and trapping sediments such as heavy metals and other pollutants in water using their dense roots and vegetation. This prevention of contaminated sediments flowing upstream can help waterways downstream (Commission, 2017). Mangroves also act as a coastal defence mechanism for many communities, as they act as buffer zones against erosion, storm surges, sea-level rise as well as other climate change events occurring along the coast, and in turn protect communities.

Salem & Mercer (2012; Kovacs et al., (2008) highlighted how mangroves help fisheries by acting as a nursery and spawning grounds habitat for fishing. This commercially supports fisheries and marine productivity; furthermore, they are tourist attraction sites as their services, such as recreational hiking, commercial fishing, commercial hunting, and bird watching, provides a source of income. Eleanya et al., (2015) outlined the importance of the mangrove ecosystem indicating that their rattan, bamboo, fibres and wood are used for making furniture and fuelwood essential for food processing and honey production.

2.4. IDENTIFICATION OF MANGROVES USING REMOTE SENSING TECHNIQUES

The use of satellites in studying different vegetation, including forest phenomenon, has been done since the early days of remote sensing. Such studies had limited access to satellite data back then, and it came at a cost. However, as more data gradually became freely available from the different sensors, more research on forest and vegetation began to occur. One sensor whose data was made available at no cost was the Advanced Spaceborne

Thermal Emission and Reflection Radiometer (ASTER) satellite system. This satellite provides a wide range of spectral coverage with fourteen spectral bands ranging from visible to thermal infrared bands with medium spatial, spectral and radiometric resolution.

The spatial resolution of ASTER makes it possible to distinguish diverse surface resources, minimizing problems while interpreting some lower resolution data resulting from mixed pixels (Crocetto & Tarantino, 2009). ASTER is a Japanese multispectral sensor system launched on-board the Terra satellite in December 1999 by NASA.

Vaiphasa et al., (2006) investigated the relationships for improved mangrove mapping using ancillary data (i.e. soil pH) as a post-classifier in a GIS map format and chose the geo-statistics interpolation for soil pH for map production. Using soil ph. as a post classifier was because mangrove species have a likelihood to be found in a particular variety of pH ratios and used the ordinary kriging method as an interpolation method based on a spherical model. The satellite imagery used ASTER for the dry season on 6 March 2002 and used a maximum likelihood classifier (MLC) in which the classifier had training samples of 260 plots. There were 263 independent samples used to test the confusion matrix calculation, which was executed using ENVI v.3.6, this is commercial software. MLC produced seven-rule maps, which contained information that can be converted to Chi-square likelihood based on mangrove species and a classified image. The overall accuracy achieved from the method was between 76.04% and 88.21%.

On the other hand, Giri & Muhlhausen (2008) used GeoCover images for 1975 and ASTER images for 2005, respectively. The GeoCover data acquired for the Multispectral Scanner (MSS), Thematic Mapper (TM) and Enhanced Thematic Mapper Plus (ETM+) was to delineate cloud-covered areas from Earth Resources Observation and Science (EROS). The study used 39 ASTER VNIR, 13 MSS, 14 TM and 16 ETM scenes, which change detection was generated by subtracting the classification maps 1975s–the 1990s, 1975s–2000s, 1975s–2005s, 1990s–2000s, 1990s–2005s, and 2000s–2005s. The areas of change detected were visually interpreted for identification of factors that may be responsible for such changes. The study used a hybrid supervised and

unsupervised classification approach to calculate mangrove and non-mangrove areas utilizing the rate of change for each period rate of change using the following formula:

Rate of change R = {1/t2-t1}1n {Ai2/Ai1}

R = rate of deforestation (area/year), A1= area at an initial time t1 and A2= area at a later time t2. Accuracy Assessment for the classified mangrove map of 2005 (ASTER) was performed using selected random points of 176, consisting of 88 sample points for mangrove classes and 88 sample points for non-mangrove classes. Their results showed that Madagascar had lost about 7% of mangrove forests from 1975 to 2005, to the extent of ~2,797 km2. The causes and deforestation rates varied both spatially and temporally. There was a 5.6% (212 km2) forest increase from 1975 to 1990, a decrease of 14.3% (455 km2) from 1990 to 2000, and a decrease of 2.6% (73 km2) from 2000 to 2005.

An example of a relationship between a biophysical variable to a spectral index is demonstrated by Jean-Baptiste & Jensen (2006); the study used ASTER imagery by correlating measurements of canopy closer taken in-situ and leaf area index (LAI) with that of the Normalized Difference Vegetation Index (NDVI) and the Soil Adjusted Vegetation Index (SAVI). The study discovered that spectral indices were positively correlated (0.851 and 0.908) with both biophysical variables. However, the study's main drawback was using a single date image. Using a single image gives limited results and fails in demonstrating if there is an established relationship with spectral indices over time. On the other hand, the advantage of using multiple date images is that if there is a relationship between biophysical variables and spectral indices, it can be verified using different dates and different study sites.

2.5. CLASSIFICATION METHODS FROM ASTER

2.5.1. Unsupervised classification

Unsupervised classification is the type of image classification where pixels are grouped into "clusters" based on their properties. After that each cluster is classified with a land cover class. In this classification, the analyst must not have samples to classify; the analysts generate clusters and assign classes before

classification. Many studies have applied this primary type of image classification, such as Marçal et al., (2005); the study used the ASTER sensor to produce updated land cover maps for the Vale do Sousa region in Brazil to segmented objects. Several classification methods used were carried out using a set of validation sites. Hierarchical clustering is a technique used on unsupervised classification data to evaluate the similarities between the land cover classes' spectral signatures. The results showed that unsupervised classification with hierarchical clustering in most classes was of several clusters in the multispectral space and that some of the classes shared the same clusters.

Koch et al., (2003) applied the same method based on the ISODATA algorithm on ASTER images; the study also used Spectral Angle Mapper (SAM), a supervised classification method. However, the ISODATA was still more useful for a generalized classification than the SAM. SAM measures the likelihood between image pixel vectors and reference vectors defined by the user, while the unsupervised classification was the most convenient method since not much required input from the user, and this could be used in cases where there was insufficient field data to be supported. This was evidence that unsupervised classification was the preferred method to be used, more especially if there was no prior knowledge of the area's characteristics under investigation and that raw image data could be converted into useful information, thus achieving higher accuracy.

2.5.2. Supervised classification

Supervised classification is the type of image classification where the analyst of an image creates training samples for each land cover class first and then the software uses these “training sites” and applies them to the entire image. This method is more suitable than the above-mentioned method, “unsupervised classification”, because this method is flexible in such a way that the training datasets contain predictor variables that measure each sampling unit, and this assigns prior classes. Even if there is the addition of new data to the classes there is no impact on the classifier. Many studies have applied supervised classification techniques on ASTER data to map and monitor vegetation in many parts of the world.

Some studies used ASTER data only, while other studies used a hybrid approach of ASTER and different satellite images. An example of such a study conducted by Barakat et al., (2018), where ASTER and Sentinel-2A images were acquired for 2001 and 2015 to monitor and analyze forest cover's spatial and temporal dynamics in the eastern area of Beni-Mellal Province in Morocco. The study applied the supervised classification method to multi-temporal images to map the different types of forest stands. The study outcomes achieved an overall classification accuracy of 97.76 and 95.80% in 2001 and 2015 images, respectively. Their results showed that an overall forest cover change had an increase in the forested area and that all species stands indicated expansion at the expense of the bare ground and crops & other classes. The use of ASTER images in mapping and monitoring vegetation, including mangroves, is a secondary objective of the ASTER sensor built for geological application, hence the number of bands in the SWIR. However, such capabilities also benefited scholars in understanding vegetation phenology within the SWIR region.

Gao & Liu (2008) used both Landsat ETM+ and ASTER data and supervised classification to compare the role of spectral and spatial resolutions in mapping land degradation (in the form of salinization and waterlogging). The results showed that the accuracy achieved was 56.8% and higher for moderately degraded (e.g., salinized) farmland and over 80% for severely degraded land (e.g., barren) from both ASTER and ETM+ data. The study also showed that the eight bands 30m ETM+ outperformed the 14-band ASTER image of 15m and 30m resolution, consistently generating a higher overall accuracy. This researcher questions the outcomes of the study based on the following, “How did the authors come to such a conclusion where an eight-band lower spatial resolution sensor could outperform a fourteen-band higher spatial resolution”?

Another study by Akumu et al., (2010) used ASTER and Landsat ETM+ and Landsat TM satellite imageries to map and monitor the coastal wetland communities in north-eastern New South Wales (NSW) Australia. The study used supervised classification by employing the maximum likelihood standard algorithm. The study successfully classified wetlands with an overall accuracy of 72.65%. However, the study was not specific on which sensor achieved better accuracy in delineating the wetlands; it could only be an assumption that a higher resolution sensor gave the better results and, in this case being ASTER.

2.6. DIFFERENTIATION TECHNIQUES USING VEGETATION INDICES

2.6.1. Normalized Difference Vegetation Index

Normalized Difference Vegetation Index (NDVI) and Soil Adjusted Vegetation Index (SAVI) have been used to monitor and map vegetation cover, biomass cover and vegetation extent. NDVI has helped in drought monitoring and agricultural production as it helps with green vegetation, while SAVI minimizes soil brightness influence using the soil-brightness correction factor to see vegetation coverage. Many studies have adapted these techniques, and they successfully worked and produced favourable results. Among those studies done by Rouse et al. (1974) it was established that NDVI was capable of monitoring vegetation cover and is the ratio of the difference in the Near Infrared and Red light, respectively. This index behaved so that green vegetation has strong reflectance in the NIR and strong absorption in the red band in the visible region with values ranging between -1 and +1. The positive value then corresponds to vegetated areas, while the negative values correspond to non-vegetated areas (Yengoh et al., 2014). Such a discovery has led to many studies where different vegetation species identified and discriminated from neighbouring land cover using this exact method.

As much as NDVI had earlier proven to be successful in vegetation discrimination studies, it became apparent that it did have background noise and saturation limitations. Therefore, the development of the Soil Adjusted Vegetation Index (SAVI) was to improve such constraints. It was first reported by Huete (1988) that SAVI minimized the effects of soil brightness and was less affected by the types of soil background (Panda et al., 2010).

While Maryantika & Lin (2017) supported these findings by confirming that SAVI was an index designed to compensate for soil background effects on NDVI, these effects showed linearly related red and infrared reflectance values and could be moderately controlled by a correction factor L. This factor had three values representing different canopy backgrounds: L = 0.25 for higher vegetation density in the field, L = 0.5 for intermediate vegetation density and L = 1 for the low vegetation density. Huete (1988) recommended that SAVI L = 0.5

successfully decreased the influence of soil differences in green vegetation compared to NDVI.

Maryantika & Lin (2017) in Sidoarjo District in East Java Province, used multi-temporal Landsat images for deriving information in the LULC (Land Use Land Cover) maps by using indices such as GNDVI (Green Normalized Difference Vegetation Index), NDVI and SAVI due to mangrove change distribution in the area. From 1995 to 2015, 25% of cropland and 15% of bare land changed to become built-up areas, 8% of wetland and 22% of mangroves changed to cropland, which led to mangroves remarkably decreasing in the district. The accuracies of the indices were close to one another, and the average GNDVI performance for the LULC type for five images had a kappa of 0.33 ± 0.10 for the specific five images, and NDVI and GNDVI were very close to each other by NDVI at 0.29 ± 0.12, while SAVI was at 0.31 ± 0.12. Therefore, the study demonstrated that SAVI produced better results than NDVI, even though the height of vegetation was not mentioned in the study because, NDVI tends to saturate in dense vegetation canopies. SAVI works well in low vegetation areas with less dense vegetation.

Sari & Rosalina (2016) did another study, mapped and monitored mangrove density changes due to the tin mining area of Bangka Belitung. The study used Landsat image data for the years 1997, 2009 and 2014; and used NDVI for mangrove analysis. The results showed that the overage mangrove area dropped from 2,807.79 ha in 1997 to 1,596.38 ha in 2014. Overall, percentages of the mangrove coverage area showed a decline over the timeframe, overall accuracies of 86.8% to 34.3% from sparse class, a slight drop in the middle class from 13% in 1997 to 10.7% in 2014 with an increase in dense class with a percentage from 0.29% to 55.0% in 2014. However, the study did not use other indices to monitor the density or correlate NDVI to other indices for more detailed analysis.

Another application of multispectral satellite data is evident in (Ibharim et al., 2015; Roslani et al., 2014); both studies used three multispectral satellite data: Landsat TM 1993, Landsat ETM+ 1999 and RapidEye 2011. The study generated a false colour composite of the Matang Mangrove Forest using 5, 4, 3 for RapidEye and 4, 5 and 3 for Landsat band combinations (Ibharim et al.,

2015), together with supervised classification and Normalized Difference Vegetation Index (NDVI) to map vegetated and non-vegetated areas.

While (Roslani et al., 2014) integrated the Normalized Difference Vegetation Index (NDVI) by using NDVIRed and $NDVI_{Red\ Edge}$ with Maximum likelihood Classifier (MLC) for classifying mangrove vegetation. However, the study found out that there was a decline in the mangrove area due to conversions of water bodies at 2490.6 ha (31.1%), dryland forest at 2456.6 ha (30.6%), Oil plantation at 1518.6 ha (18.9%), aquaculture at 890.7 ha (11.1%), paddy plantation at 391.1 ha (4.9%), horticulture at 245.6 ha (3.1%), and urban settlement area at 24.1 ha (0.3%).

Spatiotemporal changes and distribution in mangrove forest are investigated by (Chen et al., 2013; Dan et al., 2016); both studies used Landsat imagery to map the extent of the current mangrove forest in the Sundarbans Delta, and in the West and Central Africa (Dan et al., 2016) and Honduras (Chen et al., 2013). Both studies found out that there was a rapid loss in the mangrove forests. The 28-year period (1985-2013) in Honduran lost approximately 11.9%, while in West and Central Africa, mangrove loss from 1988 to 2014 was about 16.9%, and in the Sundarbans Delta, there was a remarkable increase of approximately by 15.3%.

(Kanniah et al., 2015; Omar et al., 2018) successfully mapped mangrove deforestation rates in Malaysia. Both authors utilized Landsat imagery for different periods; Omar et al., (2018) used the Random Forest classifier with vegetation indices like Green Atmospherically Resistant Index (GARI), Normalized Different Vegetation Index (NDVI), and Normalized Difference Infrared Index (NDII) for the years 1990, 2000 and 2017. The study found out that mangroves shrunk from 1990 to 2017 by about 793 ha yr-1 or 0.13% yr-1. While Kanniah et al., (2015) used Maximum Likelihood Classification (MLC) and the Support Vector Machine (SVM) technique from 1989 to 2014 period and the results yielded that there was indeed a rapid decrease of 33%.

The ability of CASI-2 hyperspectral data was assessed by Kamal & Phinn (2011) to map mangrove vegetation using pixel-based and object-based approaches in South East Queensland, Australia, at the mouth of the Brisbane River area. They

used multi-scale segmentation for the object-based image analysis (OBIA) while using spectral angle mapper (SAM) and linear spectral unmixing (LSU) for the pixel-based approaches. The results showed an accuracy of 69% for SAM, 56% for LSU and 76% for OBIA. However, the study does not reveal the extent of mangroves and whether they are increasing or decreasing. Meanwhile Phinn & Duke (2007) compared the time series analysis using NDVI on Landsat imagery and aerial photographs for Pioneer River Estuary near Mackay, Queensland, Australia, to map changes caused by natural and anthropogenic changes in mangrove area between 1948 and 2002. The results indicated that there was a loss of 137 ha (22%). However, the study does not detail what is better at documenting mangroves changes between aerial photographs and Landsat imagery.

An example of how the tidal effect can influence mangrove mapping is evident in Zhang et al. (2017). They used the Decision Tree algorithm and Multitidal Landsat 5 Thematic Mapper (TM) data and a Digital Elevation Model (DEM), With Normalized Difference Moisture Index (NDMI), the Normalized Difference Vegetation Index (NDVI) and NDVIL·NDMIH (the multiplication of NDVIL by NDMIH, L: low tide level, H: high tide level) to map mangroves collected at a single-tidal event in Fang Chenggang City, China. The results demonstrated that spectral signatures of mangrove forests influence image acquisition at different tide levels; thus, it could not yield any accuracy if a single-tidal event is used to map mangrove forests, particularly those acquired at high tide.

Suwanprasit (2018) compared five vegetation indices: Normalized Different Vegetation Index (NDVI), Simple Ratio (SR), Soil Adjusted Vegetation Index (SAVI), Perpendicular Vegetation Index (PVI) and Triangular Vegetation Index (TVI), for 2010; to explore which one would be ideal in delineating mangrove areas in Pa Khlok sub-district, Phuket, Thailand, using THEOS (Thailand's first Earth Observation Satellite). The study outcomes indicated that the optimum obtained results of 96.78%. The reason for this is because the indices we merged with the four spectral bands of the sensor to increase classification information, Figure 2. However, the authors did not discard each index's performance; they indicated that the individual indices performed well, as seen in (Table 1) below.

Table 1: Performance of individual indices and when merged with satellite THEOS, spectral bands.

The overall accuracy and Kappa coefficient of the classification.

Inputs	Overall accuracy	Kappa coefficient
THEOS 4 Bands	96.46%	0.95
THEOS 4 Bands+ NDVI	96.78%	0.96
THEOS 4 Bands + SR	96.78%	0.96
THEOS 4 Bands + SAVI	96.78%	0.96
THEOS 4 Bands + PVI	95.67%	0.94
THEOS 4 Bands + TVI	95.30%	0.94
NDVI	87.60%	0.66
SR	92.38%	0.77
SAVI	87.60%	0.66
PVI	64.71%	0.32
TVI	83.05%	0.57

The results as indicated in (Table 1) above show that the indices achieved higher accuracies when merged with satellite, and the merged best indices that achieved high accuracies were THEOS 4 Bands + NDVI, THEOS 4 Bands + SR and THEOS 4 Bands + SAVI, while these bands also performed better even when not merged with the satellite bands. This is a clear indication that for mapping exercises performed better with satellite data.

2.6.2. Leaf Area Index

The leaf area index (LAI) is a mathematical equation used to quantify plant canopy. It has been used in several remote sensing studies involving biomass monitoring and prediction, net primary production, aboveground biomass, and canopy height. Aboelghar (2011) termed LAI as the overall one-sided foliage extent per unit surface area, and it is the most significant biophysical parameter in distinguishing canopy. While Scurlock et al., (2001) defined LAI as the amount of leaf area in a vegetation canopy per unit land area. Like net primary, LAI is a key structural characteristic of vegetation and land cover because of the role of green leaves in a wide range of biological and physical processes. Fei et al., (2011), defined LAI as a quantitative variable that can be used to analyze energy exchange in the mangrove ecosystem and be used in mangrove biomass estimation and pest evaluation. Kovacs et al., (2005) estimated LAI based on an NDVI map using IKONOS and in-situ LAI-2000 sensor data for the Agua Brava Lagoon, Mexican Pacific. The results showed that the combination of IKONOS satellite data and the LAI-2000 could be used to map LAI at the species level.

However, the study only used in-situ data without comparing LAI measured from the satellite, but that depends on the author's objectives and preferences.

The use of UAV image to map mangrove LAI is described in Tian et al., (2017). They used WorldView-2 image (WV2) and compared it with UAV together with three representatives NDVIs, average NDVI (AvNDVI), vegetated specific NDVI (VsNDVI), and scaled NDVI (ScNDVI), were acquired with UAV and WV2 to predict the plot level (10×10 m) LAI. The results showed that AvNDVI was the most accurate with WV2, while ScNDVI obtained the best UAV accuracy. The comparison suggested that UAV received a higher accuracy than WV2, the RMSE of WV2 was 0.753, whereas UAV was 0.835. The reason for such outcomes was that UAV could effectively eliminate background influences and vegetation species because of its very high spatial resolution, as shown in (Figure 4) below.

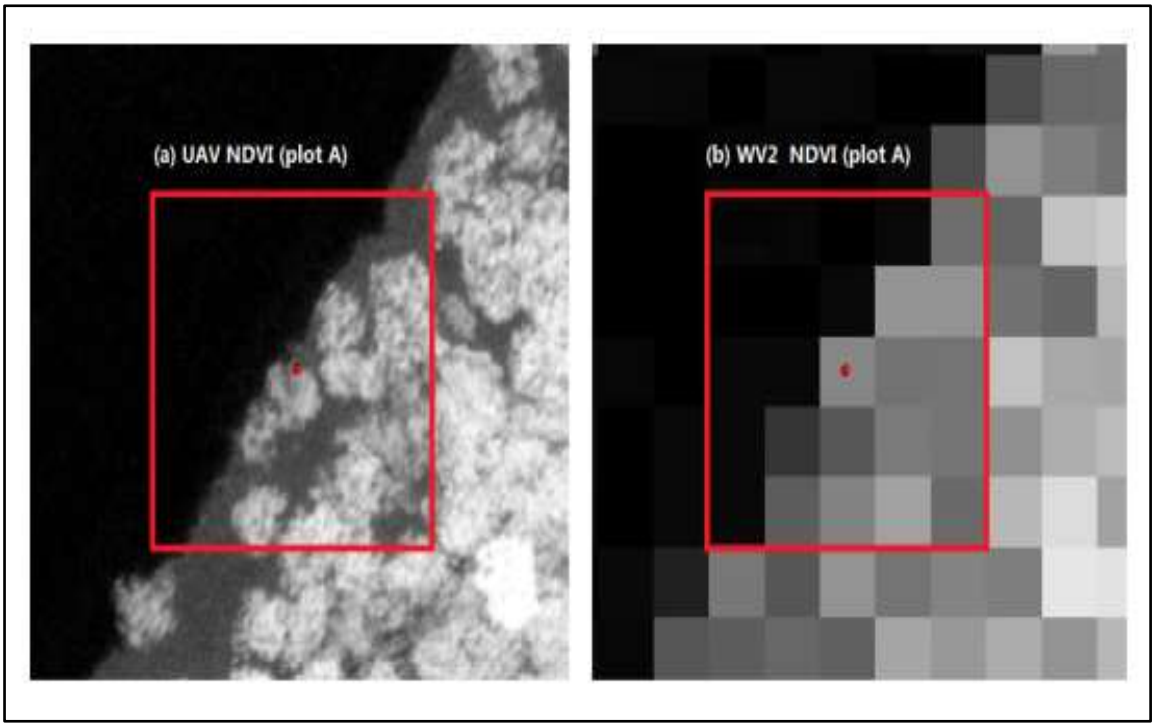

Figure 4: Comparison of pixel-level NDVI from UAV and WV2. The NDVI value is represented by an image with 256 levels of gradation, in which NDVI increased with increasing grayscale values. The red box is the boundary of plot A, and the red point is the centre of plot A. (adopted from Tian et al., 2017).

Kamal et al., (2015) investigated different mangroves effect on environmental settings using satellite image spatial resolutions, spectral vegetation indices (SVIs) and the mapping approach for LAI estimation. They compared WorldView-2 (WV-2), ALOS AVNIR-2 (AVNIR-2) and Landsat TM (TM) image data (2m, 10m and 30m pixel sizes for estimating LAI by using regression analysis at sites found in Moreton Bay (Australia) and Karimunjawa Island

(Indonesia). The results showed that LAI estimated from remote sensing data is site-specific, some mangrove habitats (i.e., homogenous versus heterogeneous stands) and that leads to LAI values having different distribution patterns, and that LAI values are not dependant on mangrove formation (i.e., scrub, low-closed forest and closed forest) instead they depend on canopy cover and mangrove phenological stages.

Flores-Verdugo investigated LAI estimation (2009); the study used the handheld AccuPAR LP-80 Ceptometer and QuickBird very high-resolution optical satellite data with 300 indirect in-situ LAI measurements obtained at various sites. Regression analyses (derived from QuickBird) of the in-situ LAI with both the normalized difference vegetation index (NDVI) and the simple ration (SR) vegetation index showed positive relationships [LAI versus NDVI (R^2 = 0.63), LAI versus SR (R^2 = 0.68)]. As much as the direct use of NDVI is for characterizing plant vigour, canopy spectral characteristics, canopy growth and changes of green leaves in plants, it is also compatible with LAI; hence studies, directly and indirectly, correlated NDVI and LAI. This also suggests that these two indices can be used to complement vegetation or forest mapping and monitoring studies such as this one.

3. CHAPTER 3: METHODS AND METHODOLOGY

3.1. DATA SOURCE AND SETS

3.1.1. ASTER Image Acquisition

ASTER (Advanced Spaceborne Thermal Emission and Reflection Radiometer) is a multispectral medium spatial, spectral and radiometric resolution on-board the Terra satellite of NASA's Earth Observing System (EOS) in collaboration with the Japan Resources Observation System Organization (JAROS). It was launched on 18 December 1999 with a sun-synchronous orbit at a local time of 10:30 am and 16-days of recurrent. ASTER was initially targeted at mapping or investigating geological interactions such as geology and soil, volcano monitoring, hydrology, etc. (Abrams, 2010; Chrysoulakis et al., 2010).

ASTER satellite imagery was selected for the study over other satellites, which are freely available such as Landsat, Sentinel and MODIS, because it possesses

higher spatial resolution properties over these satellites as mentioned above. ASTER has fourteen spectral bands, of which four bands are in the visible and near-infrared (VNIR) region at 15m resolution, while the shortwave infrared (SWIR) sensor has six bands at 30m resolution, and finally, the thermal infrared (TIR) sensor has five bands with 90m resolution. ASTER Level 1B images of Mngazana mangrove forest, acquired for 2008, 2009, 2016 and 2018; were used in this research because these were the only images available for the study area within the investigation period (Table 2).

Level-1B (L1B) is a Level-1A (L1A) data (ASTER acquires data around the whole globe with 8% average duty cycles per orbit. This means that acquisitions of 650 scenes per day are processed to Level-1A; about 150 are processed to Level-1B), with applied radiometric calibration and geometric resampled coefficients, while data in L1A is unprocessed, reconstructed, and used without the coefficients to the imagery; hence original data values are maintained (Abrams, 2010).
ASTER L1B was chosen over L1A as aforementioned because L1A has unprocessed and reconstructed data at full resolution with coefficients appended not applied, while L1B data is stored in the metadata simultaneously as an HDF file and images are radiometrically corrected.

All images were acquired with 0% cloud cover and were obtained from the USGS online data portal (http://earthexplorer.usgs.gov//). Only the VINR region with band 1, 2 and 3 where green ranges between 520–600 nm, red 630–690 nm and near-infrared between 790–860 nm respectively in the electromagnetic spectrum (Table 1). The short-wave infrared (SWIR) channels of ASTER stopped operating in April 2008 due to the cryocooler's failure (Chrysoulakis et al., 2010).

Table 2: ASTER satellite band information (Yamaguchi et al., 1998)

Spectral Region	Band No.	Spectral Range (μm)	Spatial Resolution (m)
VNIR	1	0.52-0.60	15
	2	0.63-0.69	
	3N	0.78-0.86	
	3B	0.78-086	
SWIR	4	1.60-1.70	30
	5	2.145-2.185	
	6	2.185-2.225	
	7	2.235-2.285	

	8	2.295-2.365	
	9	2.360-2.430	
TIR	10	8.125-8.475	90
	11	8.475-8.825	
	12	8.925-9.275	
	13	10.25-10.95	
	14	10.95-11.65	

3.1.2. Field Data Collection

Field sampling was carried out to collect information on the composition of vegetation types/classes. The sampling points were pinned on the map using a 'placemark' in Google Earth Pro (version 7.1.2.2041). A stratified random sampling method was used for locating the sampling plots. The GPS was used to locate field sample plots, gather location attributes of plant species and provide field-points for assessing the classification accuracy of the vegetation type map. The field validation data was collected at the Mngazana mangrove forest in November of 2018, where 139 points were selected based on accessibility and availability of mangroves. Figure 1 shows the location where the points were taken. For every point captured, the following properties were recorded on each point; Global Positioning Systems (GPS) coordinates of the survey location, the types of mangroves, saltmarshes, presence or absence of the harvested mangrove stands, open water, terrestrial vegetation, soil and bare ground.

Figure 5: Control points used in the field data collection

3.2 DATA ANALYSIS AND INTERPRETATION

3.2.1 Softwares

There were two software packages used to analyze data; one was Quantum GIS, popularly known as QGIS, and the other software was ENVI. A plugin in QGIS called Semi-Automatic Classification was used for pre-processing the images, which included atmospheric correction Dark Object Subtraction 1 (DOS1), layer stacking and subsetting of the study area. At the same time, ENVI was used for performing information extraction post-processing. This included selecting the Region of Interest (ROI), classification of land-cover classes and calculating the vegetation indices used in this study.

3.2.2. IMAGE PREPROCESSING

As data was acquired in Level 1B, it means that the data was in irradiance. Therefore, it was critical to convert the data to Top of the Atmosphere reflectance (TOA). TOA is the combination of atmospheric and surface reflectance applied to reduce the variability of the in-between-scene by normalizing solar irradiance or correction using the DOS1 (Dark Object Subtraction 1) (Congedo, 2018). This technique assumes that some of the pixels are incomplete shadows due to the

radiance received by satellite and atmospheric scattering or path radiance (Congedo, 2018). The process was also done using the “Semi-Automatic Classification plugin” (SCP). The plugin provided numerous easy to follow systematic pre-processing tools, including that of atmospheric correction, as shown in (Figure 6). Once the images were atmospherically corrected, a composite image was created by stacking all individual spectral bands. this process was also done using the Semi-Automatic Classification Plugin (Figure 6)

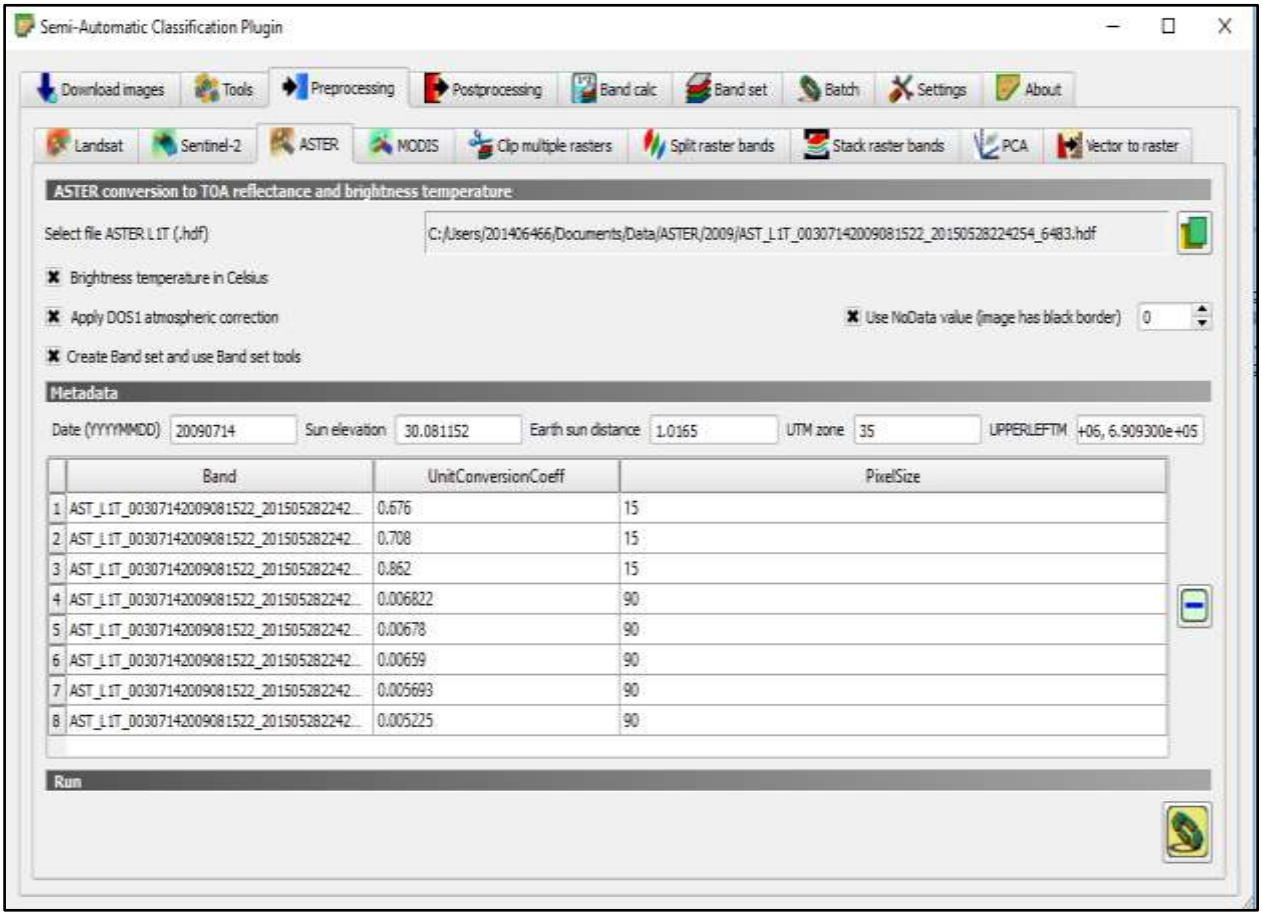

Figure 6: Graphic user interface of the Semi-Automatic Classification plugin

The QGIS software simplified this process because the entire pre-processing chain was embedded within the plugging, unlike in ENVI, where the same procedure would have been done separately, which would have increased human errors. However, ENVI software was nonetheless used for post-processing of the data. As the mangroves covered a fraction of the entire ASTER scene, the study area was extracted to maximize the processing time and focus on the mangroves' analysis and not the surrounding land cover. The Region of Interest (ROI) tool was used to subset the mangroves from the stacked images to achieve this. The methodological framework applied in this study for mapping and monitoring the mangroves of Mngazana is presented in Figure 7.

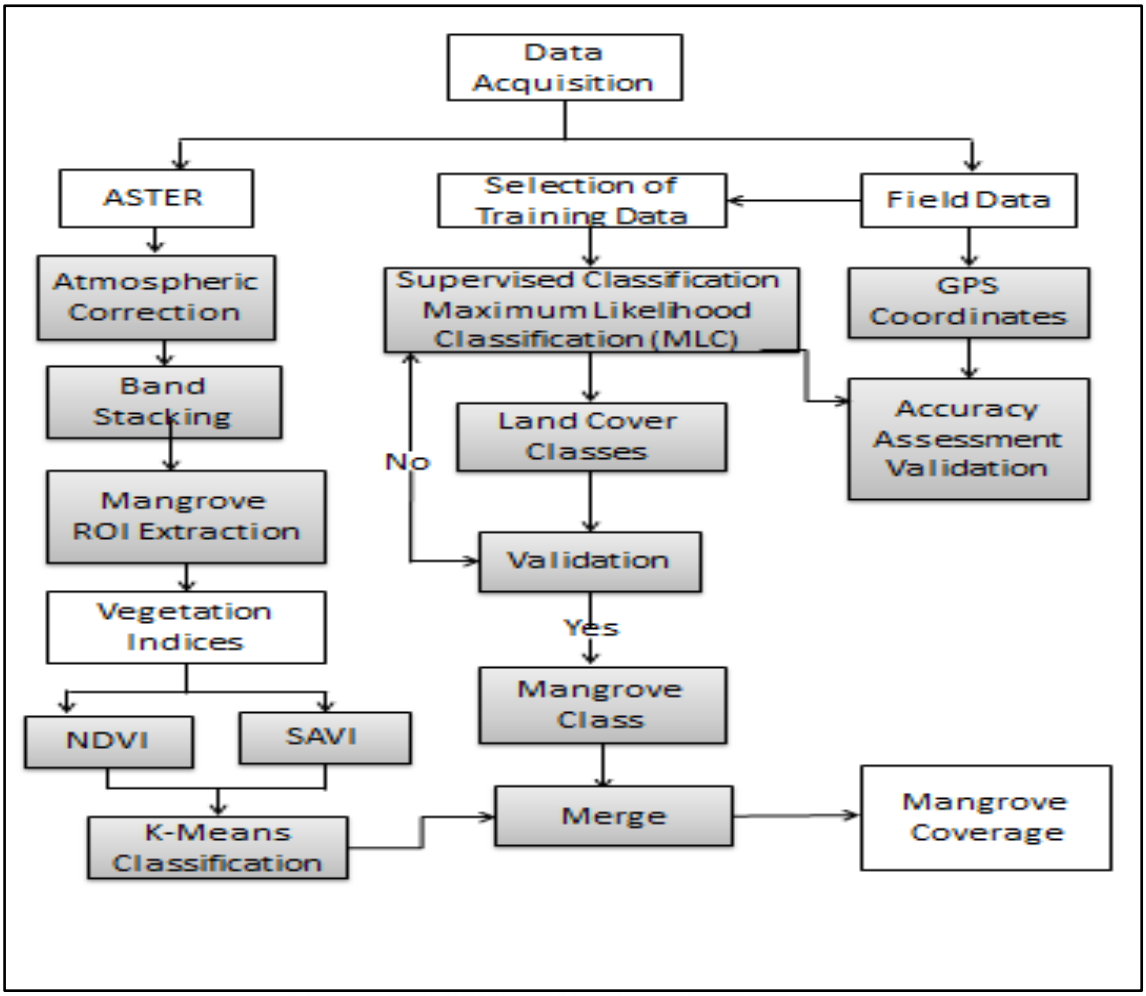

Figure 7: Methodological flowchart of the procedure used in the study

3.2.3. NDVI and SAVI Vegetation Indices

Vegetation indices attempt to minimize the impact of sources of environmental effects: soil colour, soil brightness, moisture, shadow, and upgrade the vegetation response (Ozbakir & Bannari, 2008). According to Jensen & Hardin (2005), vegetation indices are considered dimensionless radiometric measures demonstrating how abundant green vegetation activity is. In contrast, Jung et al. (2012) referred to VI as critical satellite-derived data for retrieving information on monitoring and assessing the earth's vegetation cover. Nowadays, most maps of mangrove forests are derived from remotely sensed data and represent changes in the extent and land cover. The vast majority of studies use remote sensing technologies to identify mangrove forests and measure their spatial extent.

Many methodologies have been developed to discriminate mangrove from non-mangrove vegetation. Vegetation indices are used in remote sensing studies and applications for various reasons such as; maximizing the vegetation characteristics' sensitivity and minimizing the variations in soil background

reflectance's, atmospheric effects, and illumination conditions. The functionality of the vegetation indices such as NDVI is to remunerate the impact of factors such as the spectral reflectance connection between vegetation. It is evident in the characteristics of crops, such as Leaf Area Index (LAI) and unpleasant aspects such as soil background and atmospheric effects. Distance-based vegetation indices such as SAVI reduce the soil background's impact, especially in areas where there is sparse vegetation cover; this means that the information in the image pixel contains a combination of soil and vegetation (Panda et al., 2010).

As a result, the following indices were computed in this study: the Normalized Difference Vegetation Index (NDVI) and the Soil Adjusted Vegetation Index (SAVI) as illustrated in equation 1 and 2, respectively. The affiliation is because the physiological chlorophyll *a* and *b* inside the palisade layer of healthy green vegetation leaves absorbs mostly red incident radiant flux. In contrast, the spongy mesophyll leaf layer of the near-infrared radiant flux reflects. These wavelengths bands are employed in many vegetation studies. After all, they can correlate with quantity and healthy green vegetation (Jensen & Hardin, 2005). Moreover, these can be used to monitor and access the vegetation vigour, meaning healthy vegetation can be distinguished from unhealthy plants.

NDVI was utilized to identify the mangroves' presence and absence and distinguish between the mangrove forest's vegetation types. NDVI values range from -1 (non-vegetated areas) +1 (for green, healthy vegetated areas) Barakat et al., (2018). The range of NDVI values extracted from the study area from 2008 to 2018 was from -0.29 to +0.79. The problem that NDVI has when it comes to dense aquatic vegetation is saturation; NDVI quickly reaches saturation because of its non-linearity (Brecht, 2018). The equation for calculating NDVI from remotely sensed images is represented below.

$$\text{NDVI}= \frac{Pnir-Pred}{Pnir+Pred} \quad (1)$$

Where: $Pnir$ is the near-infrared band

$Pred$ is the near red band

As discussed in Chapter 2, it was evident that SAVI plays a vital role when it comes to suppressing soil brightness, more especially in areas where there is low vegetation cover. The background of soil reflectance is easily influenced in NDVI;

thus, SAVI therefore normalizes that influence by using soil brightness correction factor. The correction factor L is adjusted depending on the quantity of vegetation, L=1; for analyzing shallow vegetation, L=0.5; for analyzing intermediate vegetation canopies and L=0.25; for high vegetation densities (Pettorelli et al., 2005). The mangrove canopy at Mngazana could be characterized as intermediate; therefore, 0.5 was used as the L factor in this study, which in most cases SAVI L=0.5) has successfully decreased the effects of soil background, as compared to NDVI (Panda et al., 2010). The selection of SAVI for this study was because it can determine plant and minimize soil effects in the study area's image.

$$SAVI = \frac{Pnir - Pred}{Pnir + Pred + L}(1 + L) \quad (2)$$

Where: $Pred$ is the brightness value from the red band

L is the soil calibration factor

In a mangrove environment, as mangroves are constantly inundated with water, the tidal height under the mangrove canopy needs attention, as an image is acquired during a high tide, the water would influence the spectral signatures of the mangroves and further compromise the classification results (Younes Cárdenas et al., 2017).

3.3. CLASSIFICATION TECHNIQUES

3.3.1. K-Means

K-means classification is a type of unsupervised classification method; this classification method was used in this study because of its computational efficiency and performance (Fang et al., 2013). This algorithm was simple as it required a specified number of classes, and in this study, since a stratified random sampling method was used for locating sample points, only ten clusters within the mangrove class were recorded using a k-means classification algorithm. These were grouped according to low, medium and high mangrove density. No sampling station plots were recorded.

3.3.2. Maximum Likelihood

Maximum Likelihood Classification (MLC) is a supervised classification method that was also used in this study because it uses parametric logic that assumes

data is typically distributed. The classes are trained based on the probability density function and use that probability to calculate each pixel that may belong to any particular class, and each pixel is assigned to the highest density (Lee & Yeh, 2009; Kanniah et al., 2015; Otukei & Blaschke, 2010). In this study, the land cover classes identified during field data collection were used as representative signatures for various land cover types specified.

Four ASTER visible near-infrared (VNIR) were used to develop the seven land cover types acknowledged in the Mngazana mangrove forest. The classification was executed in ENVI version 5.3 software using ROI (Region of Interest), a supervised classification prerequisite. For a supervised classification to be conducted, ROI (Training areas) must be selected by the user, and, it is only possible to get accurate results only if the user selects one or more ROIs of that particular land cover class identified in an image. The reason for choosing the "supervised classification technique" is that it is applied in known classes to classify the unknown regions or pixels in the image to be classified and enables the user to decide on the classes and specify the training areas, whereas the software uses these training sites to classify the images.

For this research, eight land use classes were identified. The land cover classes identified were: bare soil, mangroves, mud-banks, open water, terrestrial vegetation, salt marshes and sand, and mangroves; the focus was to classify land cover classes at Mngazana then focus only on mangroves afterwards. The purpose of field data was first to assign pixels as training samples to the image to be classified and secondly to validate the classified image. This was done so that we can be sure that what is on the image is what is on the ground, to make classification easy. This was accomplished by using the original image and the support of field data to assist the visual interpretation process for allocating each pixel type to the correct land cover class.

The natural colour was considered the best colour composite because it showed clearly land cover class units. Table 3 shows the overview of land cover classes identified during the field data collection. Supervised classification method and Maximum Likelihood Classification (MLC) were adopted in this study. The reason for using ENVI and choosing this method is because it has been the most used classification technique and delineates classes successfully with high accuracies.

For this study, a confusion matric (error matrix) was implemented to connect the ROI on the pixels used as reference using ENVI software. The matrix accurately computes each class directly, Ghebrezgabher et al., (2016a), as it assumes that samples for each class introduced to the classifier in the training stage are in a normal distribution (kavzlov 2017). According to Otukei & Blaschke (2010), the MLC works in the following way; the Maximum Likelihood Classifier calculates the following discriminant function for each pixel in the image:

$g_i(x) = -1nCOVi-(x-m_i)^t *(\text{sum over i of all } (x-mi))$
(3)

Where *i* is the class, x is the pixel, COV_i is the covariance matrix of class *i*, m*i* is the mean spectrum for class *i* (Richards 1993). ENVI calculates for each pixel the probability that the pixel belongs to a given class as probability=$g_i(x)$/ (sum over *i* of all $g_i(x)$. ENVI then assigns the pixel to the class with the highest probability. If the highest probability is smaller than the threshold value that the user enters, the pixel remains unclassified. The rule images are images of the probability calculated for each class. It is important to stress that ENVI's 'probabilities' calculated are not actual probabilities, but normalized discriminant function values Saito et al., 2003).

Table 3: Land cover classes and their description

Land cover Class	Description of Each Class
Bare soil	Areas that have no vegetation only exposed soil
Terrestrial vegetation	Areas that do not have mangroves species or coastal vegetation
Mangroves	Areas with dense mangrove tree species juvenile and adult
Saltmarsh	Areas with vegetation that is less than 1 meters tall.
Sand	Areas with no vegetation or soil, most have little or no water
Open water	Estuary main channel, rivers, streams
Mud banks	Areas of moist soils and swamps.

3.4. ACCURACY ASSESSMENT

Validation of the landcover was done by profiling each of the 139 field data points for its landcover. This process was done during the field data collection process. Furthermore, validation of the classification results is an essential step at this stage of the analysis. The process to quantify the classification accuracy was carried out using the 139 field data points sampled from the mangrove location. The overall accuracy and confusion matrix, which shows the kappa statistics, user's accuracy, and producer's accuracy, were used to evaluate the accuracy of the supervised classification carried in this study. As a result, the statistical values of the overall accuracy, kappa coefficient, omission error (producer's accuracy) and commission error (user's accuracy), were then calculated for the years at which the data was acquired, which was: 2008 2009, 2016 and 2018. The kappa statistics agree, which shows the probability values ranging from +1 to -1, respectively, representing the strongest to the most deficient agreement (Barakat et al., 2018).

4. CHAPTER 4: RESULTS AND DISCUSSION

4.1. RESULTS

4.1.1. Classification Techniques

4.1.1.1. K Means

The unsupervised k-means an algorithm was applied to SAVI and NDVI mangrove data results. This type of classification was chosen to classify the ASTER image into seven classes, as shown in Figure 8. One of those classes was the mangrove class, which was then grouped into three categories: high, moderate and low canopy density for the years 2008, 2009, 2016 and 2018.

4.1.1.2. Maximum Likelihood

The field survey conducted identified seven major land cover classes at Mngazana mangrove forest, and they were as follows: bare soil, terrestrial vegetation, mangroves, salt marshes, sand, open water and mud banks. The Maximum Likelihood (ML) classifier was used for classifying the land cover classes found at the Mngazana mangrove forest from the ASTER satellite image. The classification outcomes indicated that the Maximum Likelihood Classifier performed reasonably well with some classes; however, it did misclassify some classes such as salt marshes, bare soil and mud banks.

However, these outcomes were not out of the ordinary as the results from a study done by (Ha et al., 2018) showed similar results where MLC misclassified barren lands classes out of water bodies classes. Table 4 below shows how the land cover changed over ten years for the classes mapped.

Table 4: The estimates area of the land cover area for Years 2008, 2009, 2016, 2018

Years	Land cover Classes						
	Bare Soil	Terrestrial Vegetation	Mangroves	Salt Marshes	Sand	Open Water	Mud banks
2008	0.80	0.81	0.57	0.30	0.05	0.3	4
2009	0.18	0.99	0.09	1.71	3.60	0.45	2.7
2016	0.9	1.44	0.54	0.63	3.24	0.81	0.18
2018	0.9	0.18	0.81	1.53	89.82	0.63	2.97

Overall, the classification results were acceptable in mapping the mangrove species from 2008 to 2018. The maps produced provided information on how the mangrove forest hanged over the ten years. These changes are reflected in Figure 8.

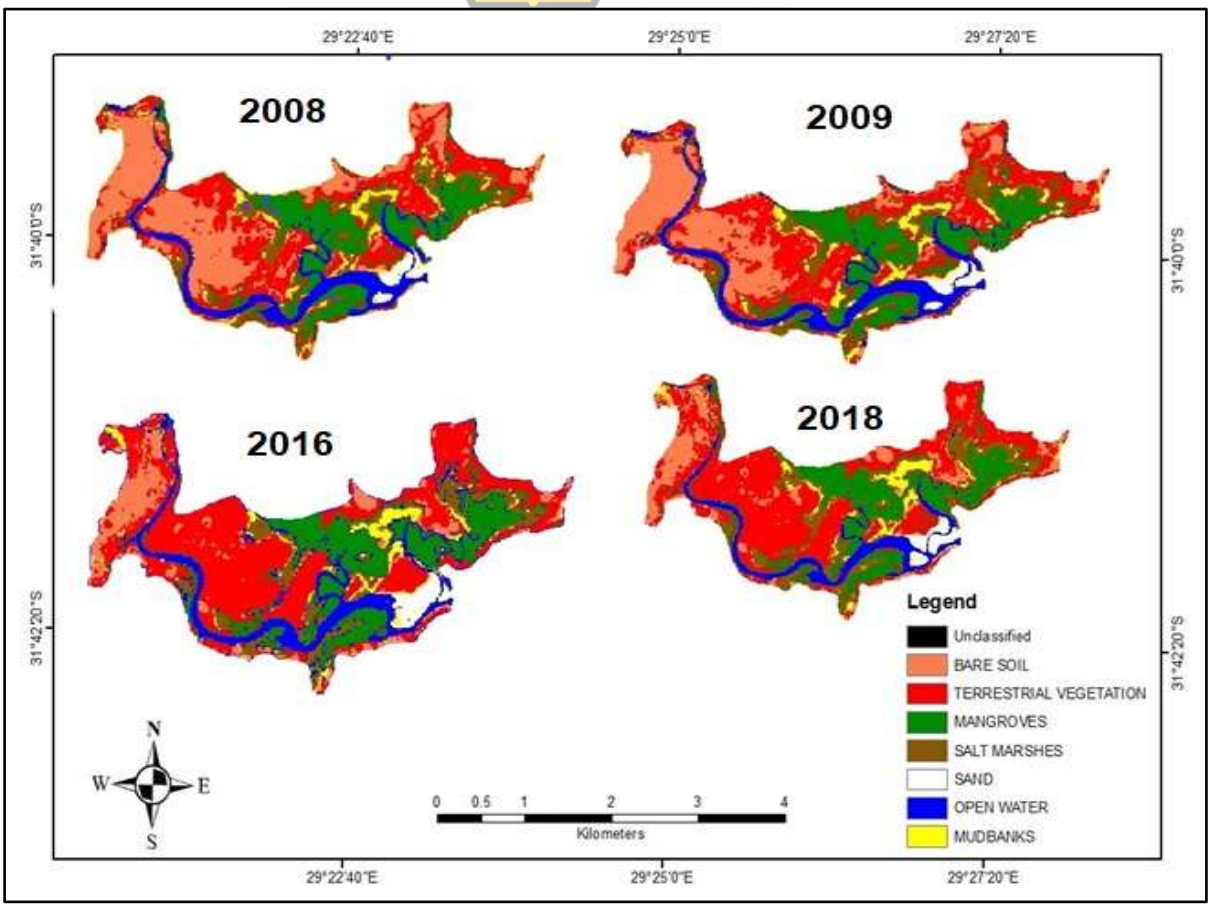

Figure 8: Shows land cover classification of the Mngazana estuary in 2008, 2009, 2016 and 2018.

4.1.1.3. Accuracy Assessment

The results obtained for the study were validated by comparing the user versus the producer's accuracies, which produced the overall accuracy and kappa coefficients. A random sampling method was adopted in this study for the accuracy assessment. A total of 139 points were randomly selected, and the outcomes for this are summarised in Table 5.

Table 5: Classified images accuracy assessment in 2008, 2009, 2016, and 2018

Years	2008	2009	2016	2018
Overall accuracy (%)	94.64	88.62	95.08	93.58
Overall kappa	0.93	0.85	0.93	0.91

Mangroves in all the years were significantly discriminated, and lower accuracies were found in the year 2009 as compared to the other years.

4.2.2. Vegetation Indices

4.2.2.1. Soil Adjusted Vegetation Index

Canopy density results for SAVI are shown in Figure 9. SAVI was used in this study to lessen the effects of soil background effects in the Mngazana mangrove forest using the soil brightness correction factor of L= 0.5, which was ideal for intermediate vegetation canopies. This index's outcomes have demonstrated that the soil brightness correction of L=0.5 was successful in minimizing the effects of soil background, which was also consistent with the study done by Panda et al., (2010).

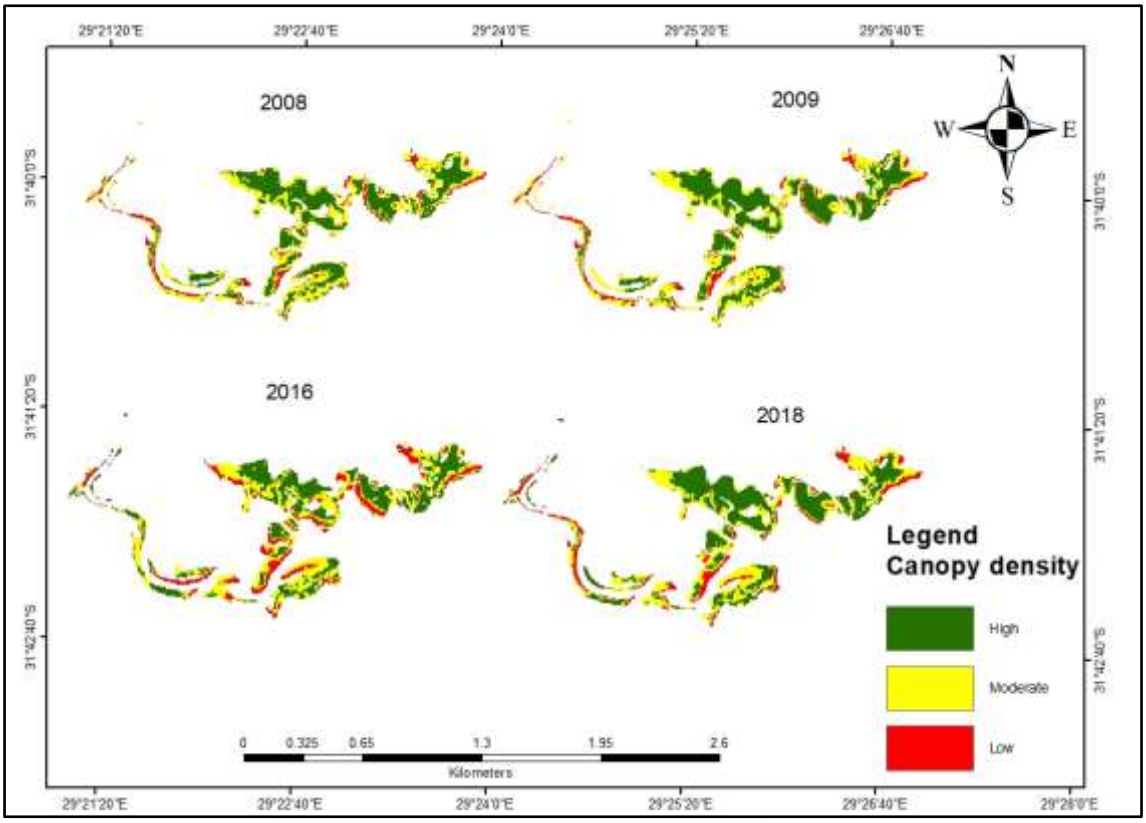

Figure 9: SAVI for mangrove density change for the years 2008, 2009, 2016 and 2018.

Figure 9 above shows the mangrove canopy density for SAVI fluctuated between the years under investigation. These changes in canopy density are well presented in Table 7 below. It is evident from the outcomes that the overall changes in the low-density canopy between 2008 and 2018 increased by 3.2% (17.3ha to 20.5ha), while the medium canopy reduced by 4.3% (60.5ha to 56.2ha) and the high-density canopy increased by 0.9% (70.4ha to 71.3ha). Interestingly, the total canopy cover between 2008 and 2018 remained at 148ha, except for a 0.2ha change. A T-test was done to evaluate whether the difference was statistically significant or not, and the outcomes indicated that the p-value was 0.33, which confirms that the total canopy changes as mapped by SAVI between 2008 and 2018 were statistically insignificant. However, this suggests that the changes in canopy density were only experienced between the canopy classes.

Table 6: Mangrove density change for SAVI and the percentages for each year

Mangrove Density Change for SAVI (ha)							
Year	Low	Medium	High	Total	Percentage (%)		
					Low	Medium	High
2008	17.3	60.5	70.4	148.2	11.5	40.9	47.6
2009	16.9	60.4	70.9	148.2	11.4	40.9	47.3

2016	27.7	59.4	61.4	148.5	18.7	40.1	41.4
2018	20.5	56.2	71.3	148	13.8	38	48.1

4.2.2.2. Normalized Difference Vegetation Index

The classified NDVI images from 2008 to 2018 show fluctuations in the mangroves' area (Figure 11). From 2008 to 2016, in the low canopy density, there was an increase of 10.2% (17.4ha to 27.4ha), and between 2016 to 2018, there was a decrease of 6.9% (27.4ha to 20.5ha). During the ten years of 2008 to 2018 there was an increase of 3.3% (17.2ha to 20.5ha). A decline of 4.4% (60.2ha to 55.8ha) in the moderate density canopy from 2008 to 2018 was observed, while in the high-density canopy, it increased by an increase of 1.3% (70.6ha) 71.9ha). However, the total mangrove cover over the years from 2008 to 2018 remains unchanged at 148ha, except for 0.13ha (Table 8). The test showed statistical insignificance with a p-value of 0.41, which suggests that the changes were experienced in the canopy densities rather than in the total mangrove coverage.

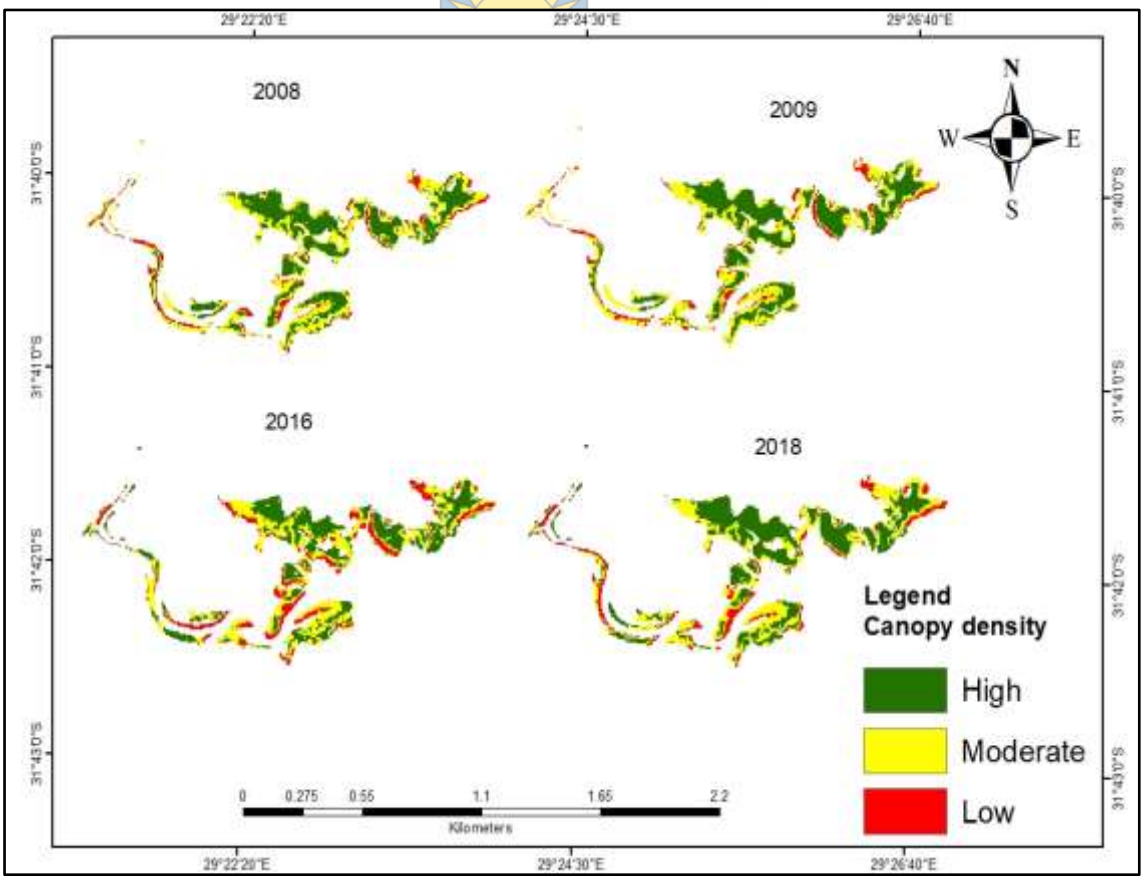

Figure 10: NDVI mangrove density change for the years 2008, 2009, 2016 & 2018

Table 7: Mangrove density change for NDVI

Mangrove Density Change for NDVI (ha)

Year	Low	Medium	High	Total	Percentage (%)		
					Low	Medium	High
2008	17.2	60.2	70.6	148	11.6	40.7	47.7
2009	16.8	61.0	69.9	147.7	11.3	41.2	47.2
2016	27.4	60.1	60.9	148.4	18.5	40.6	41.1
2018	20.5	55.8	71.9	148.2	13.9	37.8	48.5

4.3. DISCUSSION

Mangrove density changes in the Mngazana mangrove forest are mainly caused by harvesting. Overall, the mangrove coverage area remained the same 148ha throughout the ten years of this study, with the exception of 0.13ha (Table 9). However, the low-density canopy mangrove coverage in 2016 was the highest compared to 2008, 2009 and 2018.

Besides, three villages, as explained in Section 3, surround the mangrove area in Mngazana, and these villages are responsible for the decline in the mangrove density. The decline of the Mngazana mangroves could be attributed to the many years of harvesting by the locals. This was evident during the field survey where visible patches within the forest at times with mangrove stumps were seen. These observations were consistent with the mangrove poles seen left along the estuary banks (Figure 11) and some being sold as alongside the road. Fluctuations for the mangrove forest for SAVI and NDVI are shown in Figure 12 and Figure 13.

Figure 11: Mangrove poles along the river bed.

Table 9 illustrates how the total mangrove has not changed but instead, the dense canopy of mangroves for ten years (from 2008 to 2018) has changed. This change is mainly more observable in the low and high-density canopies. The reason for this is that the mangrove stands during harvesting are not cut the same because it is not monitored harvesting. Some mangrove stands are cleared adequately while others are not, this leads to those stands being categorised as low density or moderate and high density.

Apart from the mangrove stands, the mangrove seeds can regenerate and produce new mangrove trees without any form of regeneration (Geldenhuys et al., 2016). During the field trip visits, these were noticed, and during mapping, the indices picked them up but depending on their height, which will determine whether they would be classified as low, moderate or high density.

The other reason that can cause the decline observed between 2016 and 2018 is that the harvesting occurred again in the same area, and the area was big enough to be picked up by the satellite. If harvesting occurs at different places within the various densities, it cannot be easily detected, as removing for

example fifty trees at other points cannot be readily noticeable compared to the removal of 300 trees in the same area. The 0.13ha exception could be caused by the growth of mangroves in places that were cleared due to harvesting. This was confirmed by Rajkaran et al., (2004) study, which showed that the decline in mangroves at Mngazana is caused by anthropogenic activities, mainly harvesting and firewood collection which leads to the harvesting of approximately 550 trees per month which is about 1ha per year.

Table 8: Mngazana total mangrove area from 2008 to 2018

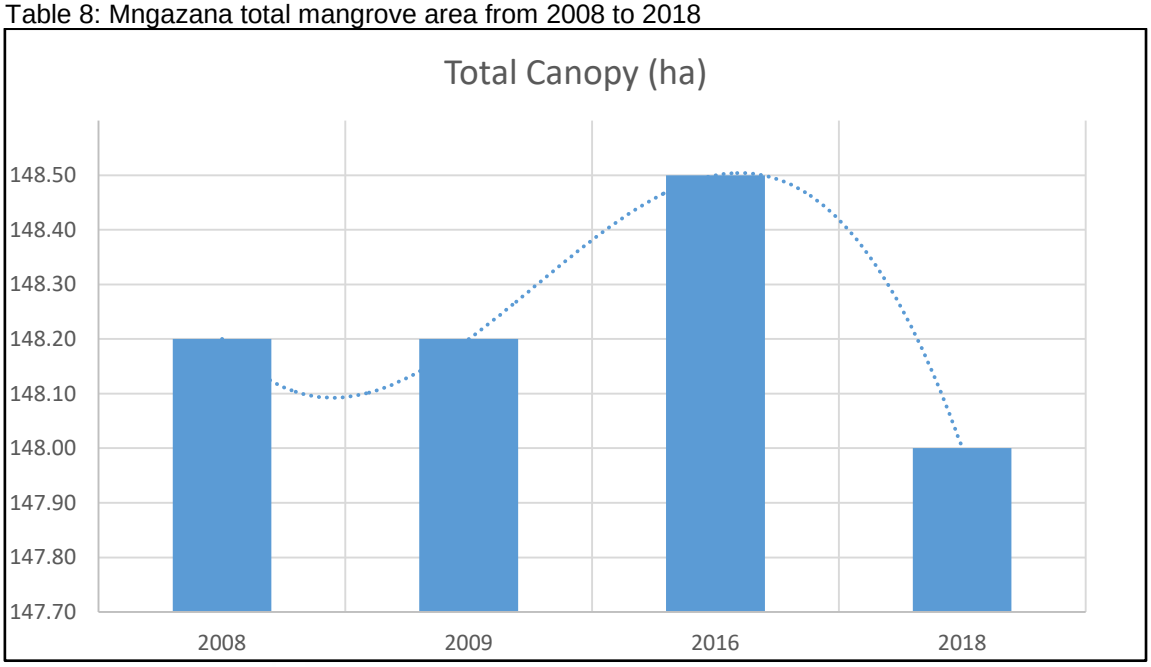

Overall, mangrove canopy coverage fluctuated over the period under investigation (2008 to 2018). There was a decrease in the moderate density canopy cover (Figure 11 and Figure 12) between 2016 and 2018 of 4.3ha. The same phenomena were also observed within the low-density canopy, where 10.2 ha were also lost. However, an increase of 11ha was observed in these indices in the high-density canopy in the same period (2016 to 2018). Percentages for moderate mangrove density canopy dipped slightly from 60.2ha in 2008 to 55.8ha in 2018. However, the high-density canopy rate rose sharply from 60.9ha in 2016 to 71.9ha in 2018, whereas there was a dip between 2008 and 2016 of 70.6ha to 60.9ha. The low-density canopy experienced a sharp rise between 2008 and 2016 of 17.2 ha to 27.4ha, and there was a sharp decrease between 2016 and 2018 of 27.4ha to 20.5ha. (Figure 12 and Figure 13).

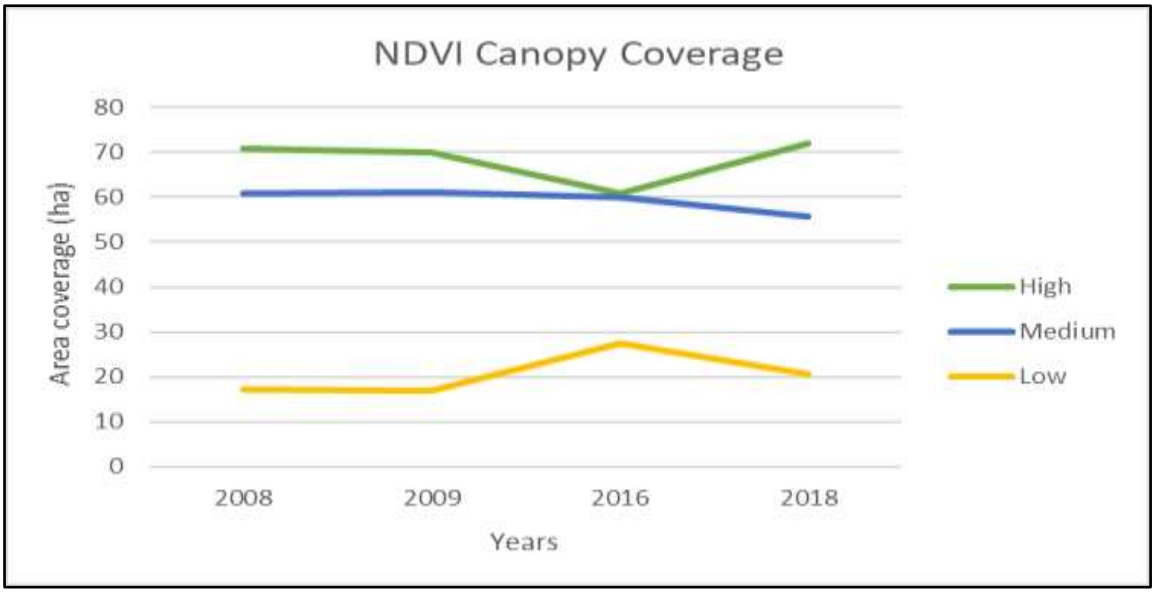

Figure 12: NDVI mangrove density cover for the years 2008, 2009, 2016 and 2018

The correlation analysis was done to determine the relationship between SAVI and NDVI for the ten years under investigation. The calculated p-value was 0.70, and based on this result, and it was evident that SAVI and NDVI were strongly correlated. As a result, these two vegetation indices were thus able to map and monitor the mangrove forest changes. These findings were consistent with a study conducted by Rhyma et al.,(2020) who obtained a p-value of 0.69 and a correlation coefficient of 0.991. At the same time, Jean-Baptiste & Jensen (2006) concluded that SAVI and NDVI were positively correlated with in-situ vegetation parameters with a correlation value of 0.908. These outcomes also confirm that SAVI and NDVI were ideal indices for distinguishing vegetated and non-vegetated areas in the area under investigation.

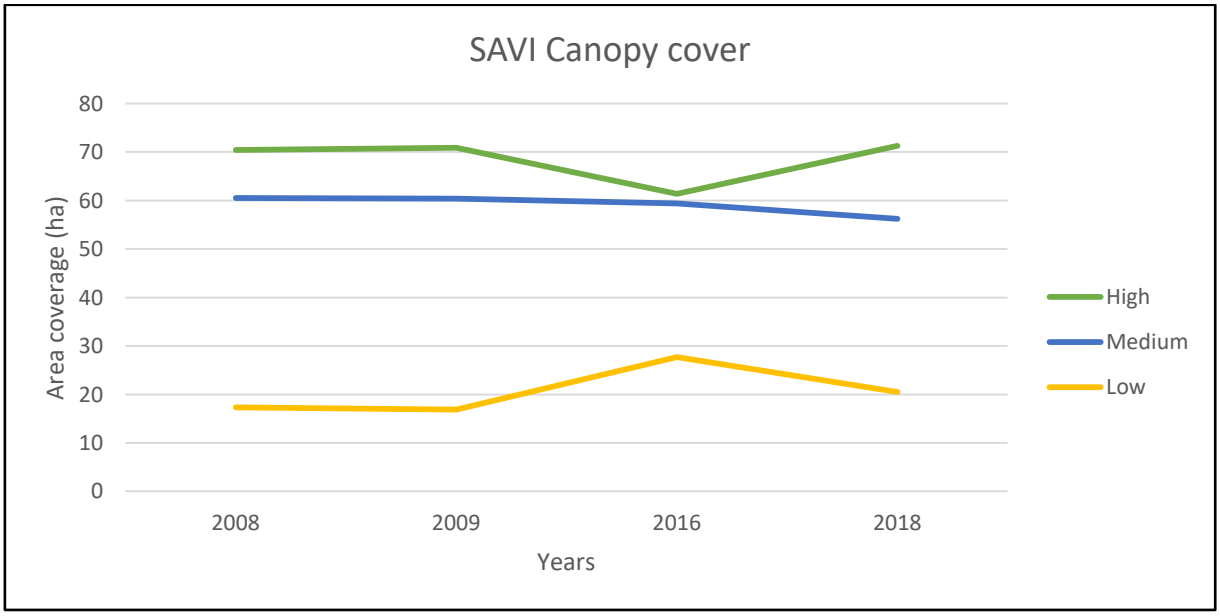

Figure 113: SAVI mangrove density cover for the years 2008, 2009, 2016 and 2018

The results indicated that the combination of biophysical variables NDVI and SAVI indices produced interesting results on mapping and monitoring mangrove canopy cover and estimating their densities. This research, like other studies, used remote sensing techniques to map and monitor mangroves, but the difference is that this research did not map and monitor mangroves at the species level as the objective of the study was not to identify the species that were declining within the forest. However, mangroves were all mapped and monitored without being discriminated amongst each other. Unlike Maryantika & Lin (2017), who used the multi-temporal Landsat TM/ETM/OLI multispectral image to compare which index between SAVI and NDVI would delineate mangroves and found out that SAVI outweighed NDVI and produced an overall accuracy of 74% and a kappa coefficient of 0.70.

Similarly Sari & Rosalina, (2016) conducted a study to monitor and measure the mangrove density changes in a tin mining area. Their research used Landsat data acquisition from the year 1997, 2009 and 2014 through NDVI analysis, and they found out that the overall percentage of mangrove coverage area declined over the timeframe. There was a significant decreased in sparse class from 86.75% to 34.31%; less change was seen in the moderate class. The percentage of moderate mangrove dipped slightly from 12.97% in 1997 to 10.66% in 2014. However, the percentage of dense mangrove rose sharply from 0.29% to 55.04% in 2014. Their study's difference is that they used only NDVI while this study used both NDVI and SAVI to map and monitor mangrove changes at the Mngazana mangrove forest.

Although the indices were able to map the mangrove change, this research's limitation would have been selecting indices that were unable to map and monitor deforestation at the Mngazana mangrove forest. This would have been a challenge, but since each method was thoroughly reviewed before it was chosen, this research had no difficulties achieving its aim. However, the deviation of this research with regards to others is aforementioned, but as mentioned before, this research extracted the mangroves from the rest of the other land cover types that are found at Mngazana mangrove forest. This was the aim because the interest was the decline in the mangrove species, not the other species found with the mangrove forest. Nonetheless, the study did not use change detection to see the rate of change in the mangroves over the years,

but it instead used the densities of the mangrove class and subdivided them into low, moderate and high. It was then within these classes that we were able to see the changes in the mangroves, that is, whether they were declining or not.

Furthermore, the changes were not due to climatic or land use but may have been influenced by the methodological consideration. However, the methodology's choice delivered valuable results, and the study did not compare which methodology amongst the others would map and monitor mangroves more than others. The obtained results established the use of remote sensing to be used for mapping and monitoring mangrove forest cover in Mngazana mangroves. The study showed that satellite-based monitoring is reliable in delineating vegetation changes when assessing the mangroves' change dynamics. Hence, the study confirms that remote sensing methodologies can provide improved forest management solutions, mainly due to the fact that satellite data is increasingly becoming freely available such as the ASTER data used in this research, which has relatively medium spatial resolution sufficient for vegetation mapping and monitoring.

5. CHAPTER 5: CONCLUSION

As the world is facing mangrove decline, more detailed, regular information on mangroves distribution and condition is required. The harvesting of mangroves at Mngazana estuary is altering the size of the forest and the population structure of the mangroves by decreasing the number of trees. If this trend continues without being monitored there will be no mangroves in the Mngazana forest in the future, it will just be bare land with stumps of cut poles and grazing field for cows. Our results illustrated how mangroves' increase or decrease could be detected and mapped using satellite-based information to guide management action and educate the local communities. This, alongside the need to assign sufficient legislative protection for ecosystems, can help slow the rate of ecosystem decline and move towards a state of recovery. The findings/results from this study could inform the local community in the Mngazana area that mangrove sustainability is crucial, especially maintaining the mangroves' health remaining to prevent the loss of mangroves. Further, the community could be involved in conducting mangrove restoration and protection

activities which could benefit from the sustainable utilization of mangrove resources by strengthening the local community's capacity to implement, monitor and report on mangrove management activities for sustainable natural resource management

Our study demonstrated the Advanced Spaceborne Thermal Emission and Reflection Radiometer (ASTER) remote sensing approach for monitoring and quantifying mangroves' deforestation in the Mngazana ecosystem. It was found that vegetation indices were able to map and monitor mangrove deforestation, and according to the results, the mangroves were not shrinking but increasing. This was due to noticeable changes in NDVI and SAVI values, although there was a decrease between 2009 and 2016 after that an increase was seen in the results of 2018. Land cover classes were classified into seven classes; bare soil, terrestrial vegetation, mangroves, salt marshes, sand, open water and mud banks, using the supervised classification classifier maximum likelihood; while the mangrove class were classified into three classes of vegetation canopy density; dense, moderately dense and low dense using the K-means classifier. A classification accuracy was conducted which produced acceptable results with good accuracies achieved of 94.64 with a kappa statistic of 0.93, 88.62 with a kappa statistic of 0.85, 95.08 with a kappa statistic of 0.93, and 93.58 with a kappa statistic of 0.91. Indeed the indices were positively correlated with each other, which yielded a significant relationship of 0.70. Dynamic estimation of the mangroves was not possible at Mngazana because mangrove extent and biomass were not considered during the mangroves' mapping and monitoring. This is because ASTER does not have bands that are active in the SWIR region. After all, they have stopped functioning since 2008, and the formula for calculating Leaf Area Index (LAI) involves the use of the SWIR bands. LAI has successfully mapped mangrove extent and biomass, and the study could have used another satellite but then using one satellite sensor was the focus to maintain consistency. However, in the future, I recommend that in-situ vegetation parameters be correlated with remote sensing-derived indices to see which ones will be highly correlated with each other and see which data will pick up mangrove deforestation between in-situ data and satellite-retrieved data.

REFERENCES

Aboelghar, M., 2011. Retrieving leaf area index from SPOT4 satellite data. *The Egyptian Journal of Remote Sensing and Space Sciences*, 13(2): 121–127.

Abrams, M., 2010. The Advanced Spaceborne Thermal Emission and Reflection Radiometer (ASTER): Data products for the high spatial resolution imager on NASA's Terra platform. , 1161.

Akumu, C.E., Pathirana, S., Baban, S. & Bucher, D. 2010. Monitoring coastal wetland communities in north-eastern NSW using ASTER and Landsat satellite data. *Wetlands Ecology and Management*, 18(3): 357–365.

Alongi, D.M., 2002. Present state and future of the world's mangrove forests. *Environmental Conservation*, 29(3): 331–349.

Alongi, D.M., 2008. Mangrove forests : Resilience, protection from tsunamis, and responses to global climate change. , 76: 1–13.

Alongi, D.M., Carvalho, N.A. De, Trott, L. & Tirendi, F. 2012. Uncoupled surface and below-ground soil respiration in mangroves : implications for estimates of dissolved inorganic carbon export. : 151–162.

Aschbacher, J., Tiangco, P., Giri, C.P., Ofren, R.S., Paudyal, D.R. & Ang, Y.K. 1995. Comparison of different sensors and analysis techniques for tropical mangrove forest mapping. *International Geoscience and Remote Sensing Symposium (IGARSS)*, 3: 2109–2111.

Bangman, B., 2007. Ecological and socio-economic values of Mangrove ecosystems in tsunami-affected areas : Rapid ecological-economic-livelihood assessment of Ban Naca

Barakat, A., Khellouk, R., El Jazouli, A., Touhami, F. & Nadem, S. 2018. Monitoring of forest cover dynamics in the eastern area of Béni-Mellal Province using ASTER and Sentinel-2A multispectral data. *Geology, Ecology, and Landscapes*, 2(3): 203–215. http://doi.org/10.1080/24749508.2018.1452478.

Blanco, A., 2013. Remote Sensing Techniques for Monitoring Aquatic Vegetation. (January).

Branch, G.M. & Grindley, J.R. 1979. Ecology of Southern African estuaries. Part XI. Mngazana: a mangrove estuary in Transkei. *South African Journal of Zoology*, 14: 149–170.

Brecht. 2018. Remote Sensing Indices. *Medium*: 1–15. https://medium.com/regen-network/remote-sensing-indices-389153e3d947.

Chen, Chi-farn, Son, N., Chang, N., Chen, Cheng-RU, Chang, L., Valdez, M., Centeno, G., Thompson, C.A. & Aceituno, J.L. 2013. Multi-Decadal Mangrove Forest Change Detection and Prediction in Honduras, Central America, with Landsat Imagery and a Markov Chain Model. : 6408–6426.

Chrysoulakis, N., Abrams, M., Feidas, H. & Arai, K. 2010. Comparison of atmospheric correction methods using ASTER data for the area of Crete, Greece. , 1161.

Chrysoulakis, N., Abrams, M., Feidas, H. & Arai, K. 2010. Comparison of atmospheric http://doi.org/10.1080/24749508.2018.1452478

Commission, G.E. 2017. Ecological Benefits. : 1–2.

Congalton, R.G. & Green, K. 1999. the ACCURACY of REMOTELY SENSED DATA Principles and Practices.

Congedo, L., 2018. Semi-Automatic Classification Plugin Documentation.

Dan, T.T., Chen, C.F., Chiang, S.H. & Ogawa, S. 2016. MAPPING and CHANGE ANALYSIS in MANGROVE FOREST by USING LANDSAT IMAGERY. *ISPRS Annals of the Photogrammetry, Remote Sensing and Spatial Information Sciences*, 3(July): 109–116.

Donato, D.C., Kauffman, J., Murdiyarso, D., Kurnianto, S., Stidham, M. & Kanninen, M. 2011. Mangroves among the most carbon-rich forests in the tropics. *Nature Geoscience*, 4: 293–297.

Duke, N.C. & Larkum, A.W., 2019. Mangroves and Seagrasses – an impression. (February).

Eleanya, K., Agbeja, B.O. & Ijeomah, H.M., 2015. Socio-Economic Importance of Mangrove Forests In Akassa Island of Niger Socio-Economic Importance of Mangrove Forests In Akassa Island of Niger Introduction Mangrove forests are increasingly recognized as crucial ecosystems in sustaining the livelihoods. (August, 2017).

Fatoyinbo, T.E. & Simard, M., 2013. Height and biomass of mangroves in Africa from ICESat/GLAS and SRTM. *International Journal of Remote Sensing*, 34(2): 668–681.

Fatoyinbo, T.E., Simard, M., Washington-Allen, R.A. & Shugart, H.H. 2008. Landscape-scale extent, height, biomass, and carbon estimation of Mozambique's mangrove, forests with Landsat ETM+ and Shuttle Radar Topography Mission elevation data. *Journal of Geophysical Research: Biogeosciences*, 113(2): 1–13.

Fei, S.X., Shan, C.U.I.H. & Hua, G.U.O.Z. 2011. Remote Sensing of Mangrove Wetlands Identification. , 10: 2287–2293.

Flores-Verdugo, F.F.D.S.F., 2009. Evaluating the condition of a mangrove forest of the Mexican Pacific based on an estimated leaf area index mapping approach. : 137–149.

Gang, P.O. & Agatsiva, J.L. 1992. The current status of mangroves along the Kenyan coast: a case study of Mida Creek mangroves based on remote sensing. *Hydrobiologia*, 247(1–3): 29–36.

Gao, J. & Liu, Y., 2008. Mapping of land degradation from space: A comparative study of Landsat ETM + and ASTER data. *International Journal of Remote Sensing*, 29(14): 4029–4043.

Geldenhuys, C., Cotiyane, P. & Rajkaran, A. 2016. Understanding the creek dynamics and environmental characteristics that determine the distribution of mangrove and salt marsh communities at Nahoon Estuary. *South African Journal of Botany*, 107: 137–147. http://dx.doi.org/10.1016/j.sajb.2016.04.013.

Ghebrezgabher, M.G., Yang, T., Yang, X., Wang, X. & Khan, M. 2016a. Extracting and analyzing forest and woodland cover change in Eritrea based on Landsat data using supervised classification. *Egyptian Journal of Remote Sensing and Space Science*, 19(1): 37–47.

Ghebrezgabher, M.G., Yang, T., Yang, X., Wang, X. & Khan, M., 2016b. Extracting and analyzing forest and woodland cover change in Eritrea based on Landsat data using supervised classification. *Egyptian Journal of Remote Sensing and Space Science*, 19(1): 37–47. http://dx.doi.org/10.1016/j.ejrs.2015.09.002.

Ghosh, M.K., Kumar, L. & Roy, C. 2016. Mapping long-term changes in mangrove species composition and distribution in the Sundarbans. *Forests*, 7(12).

Giri, C., 2016. Observation and monitoring of mangrove forests using remote sensing: Opportunities and challenges. *Remote Sensing*, 8(9).

Giri, C., Ochieng, E., Tieszen, L.L., Zhu, Z., Singh, A., Loveland, T., Masek, J. & Duke, N. 2011. Status and distribution of mangrove forests of the world using earth. : 154–159.

Green, E.P., Edwards, A.J., Mumby, P.J., Clark, C.D. & Ellis, A.C. 1998. The assessment of mangrove areas using high resolution multispectral airborne imagery. *Journal of Coastal Research*, 14(2): 483–443.

Ha, T. V., Tuohy, M., Irwin, M. & Tuan, P. V., 2018. Monitoring and mapping rural urbanization and land-use changes using Landsat data in the northeast subtropical region of Vietnam. *Egyptian Journal of Remote Sensing and Space Science* (XXXX). https://doi.org/10.1016/j.ejrs.2018.07.001.

Held, A., Ticehurst, C., Lymburner, L. & Williams, N. 2003. Mapping marine benthic biotopes using acoustic ground discrimination systems. *International Journal of Remote Sensing*, 24(13): 2761–2784.

Hoppe-speer, S.C., 2012. RESPONSE OF MANGROVES IN SOUTH AFRICA TO ANTHROPOGENIC AND NATURAL IMPACTS Sabine Clara-Lisa Hoppe-Speer Response of mangroves in South Africa to anthropogenic and natural impacts. (December).

Hoppe-Speer, S.C.L., Adams, J.B. & Bailey, D. 2015. The present state of mangrove forests along the Eastern Cape coast, South Africa. *Wetlands Ecology and Management*, 23(3): 371–383. http://link.springer.com/10.1007/s11273-014-9387-x.

Hutchison, J., Manica, A., Swetnam, R., Balmford, A. & Spalding, M., 2014. Predicting Global Patterns in Mangrove Forest Biomass. , 7(June): 233–240.

Ibharim, N.A., Mustapha, M.A., Lihan, T. & Mazlan, A.G. 2015. Mapping mangrove changes in the Matang Mangrove Forest using multi-temporal satellite imageries. *Ocean and Coastal Management*, 114: 64–76. http://dx.doi.org/10.1016/j.ocecoaman.2015.06.005.

Jean-Baptiste, N. & Jensen, J.R., 2006. Measurement of mangrove biophysical characteristics in the bocozelle ecosystem in Haiti using ASTER multispectral data. *Geocarto International*, 21(4): 3–8.

Jensen, R.R. & Hardin, P.J., 2005. Estimating urban leaf area using field measurements and satellite remote sensing data. *Journal of Arboriculture*, 31(1): 21–27.

Jung, H., Mishra, D. & Woo, J., 2012. Remote Sensing of Submerged Aquatic Vegetation. *Remote Sensing - Applications*.

Kamal, M. & Phinn, S., 2011. Hyperspectral data for mangrove species mapping: A comparison of pixel-based and object-based approach. *Remote Sensing*, 3(10): 2222–2242.

Kamal, M., Phinn, S. & Johansen, K. 2015. Object-based approach for multi-scale mangrove composition mapping using multi-resolution image datasets.

Kanniah, K.D., Sheikhi, A., Cracknell, A.P., Goh, H.C., Tan, K.P., Ho, C.S. & Rasli, F.N. 2015. Satellite Images for Monitoring Mangrove Cover Changes in a Fast Growing Economic Region in Southern. , (Im): 14360–14385.

Kavzoglu, T., 2017. Chapter 33 - Object-Oriented Random Forest for High-Resolution Land Cover Mapping Using Quickbird-2 Imagery. 1st ed. Elsevier Inc. http://dx.doi.org/10.1016/B978-0-12-811318-9.00033-8.

Koch, M., Schmid, T., Gumuzzio, J. & Mather, P.M. 2003. Evaluation of ASTER and DAIS Data for Mapping Semiarid Wetlands in La Mancha, Spain. (June 2014).

Kovacs, J.M., Crona, B., Ainul, S., Walters, B.B. & Ro, P. 2008. Ethnobiology, socio-economics and management of mangrove forests : A review. , 89: 220–236.

Kovacs, J.M., Wang, J. & Flores-Verdugo, F. 2005. Mapping mangrove leaf area index at the species level using IKONOS and LAI-2000 sensors for the Agua Brava Lagoon, Mexican Pacific. , 62: 377–384.

Kuenzer, C., Gebhardt, S. & Vo, T.Q. 2011. *Remote Sensing of Mangrove Ecosystems : A Review.*Alongi, D.M. 2008. Mangrove forests : Resilience , protection from tsunamis , and responses to global climate change. , 76: 1–13.

Alongi, D.M. 2002. Present state and future of the world's mangrove forests. *Environmental Conservation*, 29(3): 331–349.

Alongi, D.M., Carvalho, N.A. De, Trott, L. & Tirendi, F. 2012. Uncoupled surface and below-ground soil respiration in mangroves : implications for estimates of dissolved inorganic carbon export. : 151–162.

Blanco, A. 2013. Remote Sensing Techniques for Monitoring Aquatic Vegetation. , (January).

Branch, G.M. & Grindley, J.R. 1979. Ecology of Southern African estuaries. Part XI. Mngazana: a mangrove estuary in Transkei. *South African Journal of Zoology*, 14: 149–170.

Congedo, L. 2018. Semi-Automatic Classification Plugin Documentation.

Donato, D.C., Kauffman, J., Murdiyarso, D., Kurnianto, S., Stidham, M. & Kanninen, M. 2011. Mangroves among the most carbon-rich forests in the tropics. *Nature Geoscience*, 4: 293–297.

Duke, N.C. & Larkum, A.W. 2019. Mangroves and Seagrasses – an impression. , (February).

Fang, H., Jiang, C., Li, W., Wei, S., Baret, F., Chen, J.M., Garcia-haro, J., Liang, S., Liu, R., Myneni, R.B., Pinty, B., Xiao, Z. & Zhu, Z. 2013. Characterization and intercomparison of global moderate resolution leaf area index (LAI) products : Analysis of climatologies and theoretical uncertainties. , 118: 529–548.

Geldenhuys, C., Cotiyane, P. & Rajkaran, A. 2016. Understanding the creek dynamics and environmental characteristics that determine the distribution of mangrove and salt marsh communities at Nahoon Estuary. *South African Journal of Botany*, 107: 137–147. http://dx.doi.org/10.1016/j.sajb.2016.04.013.

Giri, C., Ochieng, E., Tieszen, L.L., Zhu, Z., Singh, A., Loveland, T., Masek, J. & Duke, N. 2011. Status and distribution of mangrove forests of the world using earth. : 154–159.

Ha, T. V., Tuohy, M., Irwin, M. & Tuan, P. V. 2018. Monitoring and mapping rural urbanization and land use changes using Landsat data in the northeast subtropical region of Vietnam. *Egyptian Journal of Remote Sensing and Space Science*, (xxxx). https://doi.org/10.1016/j.ejrs.2018.07.001.

Hoppe-Speer, S.C.L., Adams, J.B. & Bailey, D. 2015. Present state of mangrove forests along the Eastern Cape coast, South Africa. *Wetlands Ecology and*

Management, 23(3): 371–383. http://link.springer.com/10.1007/s11273-014-9387-x.

Hutchison, J., Manica, A., Swetnam, R., Balmford, A. & Spalding, M. 2014. Predicting Global Patterns in Mangrove Forest Biomass. , 7(June): 233–240.

Jean-Baptiste, N. & Jensen, J.R. 2006. Measurement of mangrove biophysical characteristics in the bocozelle ecosystem in Haiti using ASTER multispectral data. *Geocarto International*, 21(4): 3–8.

Kanniah, K.D., Sheikhi, A., Cracknell, A.P., Goh, H.C., Tan, K.P., Ho, C.S. & Rasli, F.N. 2015. Satellite images for monitoring mangrove cover changes in a fast growing economic region in southern Peninsular Malaysia. *Remote Sensing*, 7(11): 14360–14385.

Lagomasino, D., Fatoyinbo, T., Lee, S., Feliciano, E., Trettin, C., Shapiro, A. & Mangora, M.M. 2019. Measuring mangrove carbon loss and gain in deltas Measuring mangrove carbon loss and gain in deltas. *Environmental Research Letters*, 14(2): 25002. http://dx.doi.org/10.1088/1748-9326/aaf0de.

Lavieren, H. Van, Spalding, M., Alongi, D.M., Kainuma, M., Clüsener-godt, M. & Adeel, Z. Securing the future of mangroves.

Lee, T.M. & Yeh, H.C. 2009. Applying remote sensing techniques to monitor shifting wetland vegetation: A case study of Danshui River estuary mangrove communities, Taiwan. *Ecological Engineering*, 35(4): 487–496.

Maryantika, N. & Lin, C. 2017. Exploring changes of land use and mangrove distribution in the economic area of Sidoarjo District, East Java using multi-temporal Landsat images. *Information Processing in Agriculture*, 4(4): 321–332.

Otukei, J.R. & Blaschke, T. 2010. Land cover change assessment using decision trees, support vector machines and maximum likelihood classification algorithms. *International Journal of Applied Earth Observation and Geoinformation*, 12(SUPPL. 1): 27–31.

Panda, S.S., Ames, D.P. & Panigrahi, S. 2010. Application of vegetation indices for agricultural crop yield prediction using neural network techniques. *Remote Sensing*, 2(3): 673–696.

Pastor-Guzman, J., Dash, J. & Atkinson, P.M. 2018. Remote sensing of mangrove forest phenology and its environmental drivers. *Remote Sensing of Environment*, 205(November 2017): 71–84. https://doi.org/10.1016/j.rse.2017.11.009.

Peter sen, J., Sack, D. & Gabler, R.E. 2010. no N t t E o R be T re pu bl is he d no N t t E o R be T re pu is. In *Fundamentals of Physical Geography*. Cengage Learning, 2010: 496 pages.

Quoc Vo, T., Kuenzer, C. & Oppelt, N. 2015. How remote sensing supports mangrove ecosystem service valuation: A case study in Ca Mau province, Vietnam. *Ecosystem Services*, 14: 67–75.

Rajkaran., A. & Adams., J. 2007. Mangrove litter production and organic carbon pools in the Mngazana Estuary, South Africa. *African Journal of Aquatic Science*, 32: 17–25.

Rajkaran, A. 2011. A status assessment of mangrove forests in South Africa and the utilization of mangroves at Mngazana Estuary By Anusha Rajkaran Submitted for the fulfilment of the requirements for the degree of Philosophiae Doctor in the Faculty of Science at Nelson Mand. , (January): 1–155.

Rajkaran, A., Adams, J.B. & Du Preez, D.R. 2004. A method for monitoring mangrove harvesting at the Mngazana estuary, South Africa. *African Journal of Aquatic Science*, 29(1): 57–65.

Rhyma, P.P., Norizah, K., Hamdan, O., Faridah-Hanum, I. & Zulfa, A.W. 2020. Integration of normalised different vegetation index and Soil-Adjusted Vegetation Index for mangrove vegetation delineation. *Remote Sensing Applications: Society and Environment*, 17(May 2019): 100280. https://doi.org/10.1016/j.rsase.2019.100280.

Sari, S.P. & Rosalina, D. 2016. Mapping and Monitoring of Mangrove Density Changes on tin Mining Area. *Procedia Environmental Sciences*, 33: 436–442.

Traynor, C.H. & Hill, T.R. 2008. Resource demand estimates for sustainable forest management: Mngazana Mangrove Forest, South Africa. *Bothalia*, 38(1): 103–110.

Younes Cárdenas, N., Joyce, K.E. & Maier, S.W. 2017. Monitoring mangrove forests: Are we taking full advantage of technology? *International Journal of Applied Earth Observation and Geoinformation*, 63(July): 1–14. http://dx.doi.org/10.1016/j.jag.2017.07.004.

Venkataratnam, L., Thammappa, S.S., Sankar, T.R. & Anis, S. 1997. Mapping and monitoring prawn farming areas through remote sensing techniques. *Geocarto International*, 12(2): 23–29.

Wang, L., Sousa, W.P. & Gong, P. 2004. Integration of object-based and pixel-based classification for mapping mangroves with IKONOS imagery. *International Journal of Remote Sensing*, 25(24): 5655–5668.

Wang, Le, Sousa, W.P., Gong, P. & Biging, G.S., 2004. Comparison of IKONOS and QuickBird images for mapping mangrove species on the Caribbean coast of Panama. *Remote Sensing of Environment*, 91(3–4): 432–440.

Yang, A.S., Riddin, T., Adams, J.B., Shih, S., Journal, S., August, N., Riddin, S.Y.T. & Shih, J.B.A.S. 2018. Predicting the spatial distribution of mangroves in a South African estuary in response to sea-level rise, substrate elevation change and a sea storm event Stable URL : http://www.jstor.org/stable/24760663 Predicting the spatial distribution of mangroves. , 18(4): 459–469.

Yengoh, G.T., Dent, D., Olsson, L., Tengberg, A.E., Tucker, C.J., Jean-Baptiste, N., Jensen, J.R., Rouse, J.W., Hass, R.H., Schell, J.A. & Deering, D.W. 2014. Monitoring vegetation systems in the great plains with ERTS. *Lund University Center for Sustainability Studies (LUCSUS), and The Scientific and Technical Advisory Panel of the Global Environment Facility (STAP/GEF)*, 1(4): 309–317. https://ntrs.nasa.gov/archive/nasa/casi.ntrs.nasa.gov/19740022614.pdf.

Zhang, X., Treitz, P.M., Chen, D., Quan, C., Shi, L. & Li, X. 2017. Int J Appl Earth Obs Geoinformation Mapping mangrove forests using multi-tidal remotely-sensed data and a decision-tree-based procedure. *Int J Appl Earth Obs Geoinformation*, 62(June): 201–214. http://dx.doi.org/10.1016/j.jag.2017.06.010.